Article

Antimalarial Activity of Piperidine Alkaloids from *Senna spectabilis* and Semisynthetic Derivatives

Marcos Pivatto,[*,a] *Luciene R. Baccini,*[b] *Abhinay Sharma,*[c] *Myna Nakabashi,*[c] *Amanda Danuello,*[d] *Claudio Viegas Júnior,*[b] *Celia R. S. Garcia*[*,c] *and Vanderlan S. Bolzani*[*,b]

[a]*Instituto de Química, Universidade Federal de Uberlândia, 38400-902 Uberlândia-MG, Brazil*

[b]*Núcleo de Bioensaios, Biossíntese e Ecofisiologia de Produtos Naturais (NuBBE), Departamento de Química Orgânica, Instituto de Química, Universidade Estadual Paulista, P.O. Box 355, 14801-970 Araraquara-SP, Brazil*

[c]*Departamento de Fisiologia, Instituto de Biociências, Universidade de São Paulo, 05508-900 São Paulo-SP, Brazil*

[d]*Departamento de Química, Instituto de Ciências Exatas, Naturais e Educação, Universidade Federal do Triângulo Mineiro, 38064-200 Uberaba-MG, Brazil*

Dando continuidade as pesquisas de identificação de metabólitos secundários com propriedades anti-infecciosas potenciais a partir de espécies de plantas dos biomas brasileiros, dois alcaloides piperidínicos (–)-cassina e (–)-espectalina foram isolados das flores de *Senna spectabilis* (sin. *Cassia spectabilis*). As estruturas destes compostos foram elucidadas a partir de dados espectroscópicos e espectrométricos. Adicionalmente, esses alcaloides foram acetilados, resultando nos derivados (–)-3-*O*-acetilcassina e (–)-3-*O*-acetilespectalina. Todas as substâncias foram submetidas ao bioensaio empregando culturas de eritrócitos, infectadas com *Plasmodium falciparum*, um teste específico para avaliação antimalárica. Dentre as substâncias avaliadas, os dois primeiros alcaloides (IC$_{50}$ 1,82 μM e IC$_{50}$ 2,76 μM) foram mais potentes que os derivados (IC$_{50}$ 24,47 μM e IC$_{50}$ 25,14 μM) em comparação com a cloroquina (IC$_{50}$ 0,30 μM), utilizada como padrão. Estes dados mostram que os alcaloides piperidínicos constituem uma classe de produtos naturais que apresenta amplo espectro de atividades biológicas, sendo portanto, importantes modelos para o planejamento de fármacos, incluindo os antimaláricos.

In our continuing work looking for new anti-infective lead compounds from Brazilian biomes, the two known piperidine alkaloids (–)-cassine and (–)-spectaline were isolated from the flowers of *Senna spectabilis* (syn. *Cassia spectabilis*). Their structures were elucidated using a combination of spectroscopic and spectrometric data analysis. Further, these compounds were acetylated yielding the derivatives (–)-3-*O*-acetylcassine and (–)-3-*O*-acetylspectaline. All compounds were screened against *P. falciparum*-infected red blood cells (RBC) in culture, aiming to identify antimalarial prototypes. Among all compounds screened, the first two alkaloids (IC$_{50}$ 1.82 μM and IC$_{50}$ 2.76 μM) were more effective than the derivatives (IC$_{50}$ 24.47 μM and IC$_{50}$ 25.14 μM) in comparison to the standard compound chloroquine (IC$_{50}$ 0.30 μM). These data show that piperidine alkaloids constitute a class of natural products that feature a broad spectrum of biological activities, and are, therefore, important templates for drug design, including antimalarial.

Keywords: piperidine alkaloids, *Senna spectabilis*, semisynthetic derivatives, antimalarial activity, *Plasmodium falciparum*

*e-mail: pivatto@iqufu.ufu.br, cgarcia@usp.br, bolzaniv@iq.unesp.br

Introduction

Malaria, a life-threatening disease caused by *Plasmodium* parasites, infects and destroys red blood cells, leading to fever, severe anemia, and cerebral malaria and if untreated may cause death. It is estimated that 3.3 billion of the world's population living in 109 countries are at risk of contracting this serious and often life-threatening disease. In recent statistics, malaria accounts for ca. 250 million clinical cases and nearly 1 million deaths each year, the great majority of which occur in children younger than 5 years of age and in young, pregnant women, which are more frequently attacked because of the lower immunological protection.[1] The global malaria map has been shrinking over the past 50 years and this disease, affecting societies, by interfering with educational accomplishments, and causing serious economic problems, remains a devastating disease largely because of widespread drug resistance.[2] Without regular monitoring and reporting of antimalarial drug resistance, the disease burden and the economic costs of malaria will rise dramatically.[1] Therefore, new drugs and a better understanding of the mechanisms of drug action and resistance are essential for fulfilling the promise of eradicating malaria. Chloroquine is the most widely used antimalarial drug, but the emergence of drug-resistant parasites is rapidly reducing its effectiveness as a single agent. It is now most effective as part of an artemisinin-based drug combination. In this case, the parasite evolved a way to pump out chloroquine before the drug could accumulate to levels that would interfere with a process known as heme polymerization (which is needed to prevent the buildup of the toxic by-products of hemoglobin metabolism).[3] Chloroquine remains effective only in Central America, where clinical studies in Honduras and Nicaragua have confirmed its 100% efficacy.[1] In an analysis based on published studies conducted in 30 countries, the median treatment failure rates were high to extremely high (19.8-100%) in all the countries except Honduras, Malawi and Nicaragua (0-1.3%). In India, monitoring of chloroquine continued until 2008 despite consistently high failure rates.[4] Quinine-resistant *P. falciparum* was first reported in 1910 in Brazil. Today this parasite is resistant in most endemic areas to the widely used blood schizonticide,

chloroquine. Many strains are resistant also to antifols (e.g., pyrimethamine, proguanil) and some are also no longer eliminated by quinine. Therefore, it is essential to search for radically new compounds, for drugs that reverse chloroquine resistance and for new strategies to impede the progress of this problem.

As part of our ongoing research project on *Senna* and *Cassia* species prospecting for new bioactive piperidine alkaloids,[5-10] a further investigation on the flowers of *Senna spectabilis* (D.C.) H.S. Irwin and R.C. Barneby (Fabaceae, Caesalpinioideae) was carried out, in the hope of finding new unusual piperidine alkaloids in an EtOH extract of these flowers and to evaluate their action as antimalarial agents. To this end, this extract was subjected to successive liquid-liquid partitioning, which yielded a chloroformic alkaloidal fraction. This fraction was chromatographed using a combination of flash chromatography followed by high-performance liquid chromatography (HPLC) separations and afforded the two piperidine alkaloids ((–)-cassine (**1**) and (–)-spectaline (**2**), Figure 1). Further, the acetyl derivatives (–)-3-*O*-acetylcassine (**3**) and (–)-3-*O*-acetylspectaline (**4**) were prepared from **1** and **2**, respectively (Figure 1), in greater amounts since on previous works they were identified as a mixture of two homologous piperidine alkaloids and **4** was isolated in very low yield from *S. spectabilis*.[6,7] These compounds were then assessed for their antimalarial inhibitory activity by means of flow cytometry screening assay.[11]

Experimental

General experimental procedures

Optical rotations were measured with a 341 LC polarimeter (PerkinElmer) at 28 °C. Melting points were recorded on a differential scanning calorimeter (DSC) TA Instruments DSC-Q10 apparatus and are uncorrected. Infrared (IR) spectra were registered on a Nicolet iS10 FT-IR spectrometer coupled with an attenuated total reflectance (ATR) accessory (the samples were pressed against a crystal of Ge). The 1D (^{1}H, ^{13}C, and distortionless enhancement by polarization transfer (DEPT)) and 2D (^{1}H–^{1}H correlation spectroscopy (COSY), heteronuclear
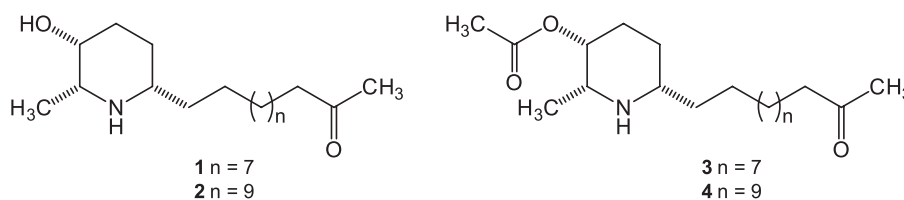

Figure 1. Piperidine alkaloids (**1** and **2**) isolated from *S. spectabilis* and (**3** and **4**) semisynthetic derivatives.

multiple quantum coherence (HMQC), and heteronuclear multiple bond correlation (HMBC)) nuclear magnetic resonance (NMR) experiments were accomplished on a Varian INOVA 500 spectrometer (11.7 T) at 500 MHz (^{1}H) and 125 MHz (^{13}C), at 30 °C, using tetramethylsilane (TMS, δ_{TMS} 0.00 ppm) as internal standard or residual solvent resonances of methanol-d_4 at δ 3.30 and 49.0 ppm or chloroform-d at δ 7.26 and 77.0 ppm, as reference for ^{1}H and ^{13}C, respectively. High-resolution mass spectra (HRMS) with electrospray ionization (ESI) were measured on an ultrOTOF$_Q$ (Bruker Daltonics) apparatus operating in the positive mode. The samples were infused into the ESI source at a flow rate of 5 μL min^{-1} and methanol/water (4:1) was used as solvent system.

Column chromatography (CC) was carried out on silica gel (70-230 mesh, Acros) and neutral alumina (70-290 mesh, Sigma). Thin-layer chromatography (TLC) was performed on silica gel F$_{254}$ plates (0.20 mm, Fluka), and spots were visualized under UV light (254 and 366 nm) and spraying with iodochloroplatinate reagent (Merck) or anisaldehyde-H$_2$SO$_4$, followed by charring for 5 min, prepared as described in the literature.[12] Analytical and preparative HPLC separations were accomplished on a Shimadzu CLASS-VP instrument equipped with a binary pump model LC-8A, a UV-Vis detector model SPD-10A*vp*, an evaporative light scattering detector model ELSD-LT, a fraction collector model FRC-10A, and an automatic sample injector model SIL-10AF and controlled with the aid of an LC workstation CLASS-VP version 6.14 SP2 software. The columns used were a Phenomenex Gemini C$_{18}$ (250 × 4.60 mm, 5 μm) and a preparative Phenomenex Synergi Hydro C$_{18}$ 80 Å Axia Packed (100 × 21.20 mm, 4 μm) protected with the corresponding guard columns. All solvents utilized in the experimental procedures were HPLC-grade or had been previously distilled. Water was purified immediately prior to use with a Millipore Milli Q plus system.

Plant material

Leaves of *S. spectabilis* were collected by M. Pivatto in Araraquara (São Paulo, Brazil), in July 2010. The plant was identified by Inês Cordeiro from Instituto de Botânica in São Paulo-SP, Brazil. A voucher specimen (SP 384109) has been deposited in the herbarium of this institute.

Extraction and isolation

The dried and powdered flowers (950.0 g) were extracted with aqueous 95% ethanol (9 L × 5) for seven days at room temperature. The solvent was removed under

reduced pressure in a rotary evaporator to yield a thick syrup (184.0 g). The crude ethanol extract (100.0 g) was reconstituted in MeOH-H$_2$O (4:1, 500 mL), filtered, and successively partitioned with *n*-hexane (250 mL × 5, 5.5 g), CH$_2$Cl$_2$ (250 mL × 5, 25.8 g), and EtOAc (250 mL × 5, 10.3 g). After removal of solvent, the CH$_2$Cl$_2$ extract (8.0 g) was subjected to CC over neutral alumina, eluting with a gradient of increasing MeOH in CHCl$_3$ (10-100%), to produce twenty fractions (F$_1$-F$_{20}$, Supplementary Information Figure S1) on the basis of TLC analysis. Fraction F$_{1-4}$ (1.76 g) was further fractionated via silica gel CC, eluting with CHCl$_3$-MeOH-NH$_4$OH (9:1:0.25), to yield two pure compounds, **1** (F$_{16-17}$, R_f 0.58, *m/z* 298, 54.8 mg) and **2** (F$_{3-4}$, R_f 0.58, *m/z* 326, 44.9 mg), and a mixture of **1** and **2** (F$_{5-15}$, R_f 0.58, *m/z* 298 and 326, 575.9 mg) on the basis of TLC and MS analysis (Figure S2). The mixture containing **1** and **2** was submitted to semipreparative HPLC on RP-C$_{18}$ and eluted with a gradient of increasing MeOH in 0.1% HOAc aqueous solution (35-100, flow rate 8.0 mL min^{-1}, 25 min), which furnished the pure alkaloids **1** (t_R 11.6 min, 120.0 mg) and **2** (t_R 15.2 min, 15.0 mg) (Figures S4-S7).

General procedure for the synthesis of compounds 3 and 4

To a solution of **1** or **2** in chloroform was bubbled a stream of hydrogen chloride gas generated in a modified Kipp's apparatus (30 min) to prepare (–)-cassine hydrochloride and (–)-spectaline hydrochloride (Figure S61).

To a solution of the hydrochloride of **1** (20.0 mg, 0.07 mmol) or **2** (20.0 mg, 0.06 mmol) in chloroform (5 mL) was added acetyl chloride (0.25 mL), and the mixture was refluxed for 4 h under nitrogen atmosphere, followed by quenching with saturated NaHCO$_3$ aqueous solution and extracted with CHCl$_3$ (10 mL × 3). The organic layer was dried over anhydrous magnesium sulfate. The dried solution was filtered and the filtrate was concentrated under reduced pressure to afford the desired products **3** (22.0 mg, 97.5% yield) and **4** (21.4 mg, 96.1% yield) as white solids.

(–)-Cassine (**1**): white solid; [α]$_D^{25}$ –0.62 (*c* 8.0, EtOH); m.p. 54.3 ºC (97.0% purity); IR (film) ν$_{max}$/cm^{-1} 3203, 2918, 2852, 1709, 1541, 1392, 1159, 1024, 957, 721, 650; ^{1}H and ^{13}C NMR data, see Table 1; HRMS *m/z* 298.2748 [M + H]$^+$ (calcd. for C$_{18}$H$_{36}$NO$_2$: 298.2746); TLC R_f 0.64 (9:1:0.25 CHCl$_3$-MeOH-NH$_4$OH).[13]

(–)-Spectaline (**2**): white solid; [α]$_D^{25}$ –3.35 (*c* 1.0, CHCl$_3$); m.p. 67.7 ºC (93.3% purity); IR (film) ν$_{max}$/cm^{-1} 3089, 2916, 2848, 1707, 1471, 1425, 1356, 1157, 1074,

993, 912, 856, 787, 719, 698, 596; ^{1}H and ^{13}C NMR data, see Table 1; HRMS *m/z* 326.3056 [M + H]$^+$ (calcd. for $C_{20}H_{40}NO_2$: 326.3054); TLC R_f 0.64 (9:1:0.25 $CHCl_3$-MeOH-NH_4OH).[6,13]

(−)-3-*O*-Acetylcassine (**3**): pale yellow oil; HRMS *m/z* 340.2852 [M + H]$^+$ (calcd. for $C_{20}H_{38}NO_3$: 340.2852); TLC R_f 0.79 (9:1:0.25 $CHCl_3$-MeOH-NH_4OH).[7]

(−)-3-*O*-Acetylspectaline (**4**): pale yellow oil; HRMS *m/z* 368.3159 [M + H]$^+$ (calcd. for $C_{22}H_{42}NO_3$: 368.3165); TLC R_f 0.79 (9:1:0.25 $CHCl_3$-MeOH-NH_4OH).[6,7]

In vitro culture of *Plasmodium falciparum* (3D7)

Parasites were cultured and synchronized as described previously.[14] In brief, parasites were maintained at 1-10% parasitemia and 2% hematocrit in Roswell Park Memorial Institute (RPMI) 1640 culture medium supplemented with erythrocytes, 10% human serum, 0.16% glucose, 0.2 mM hypoxanthine, 2.1 mM *L*-glutamine and 22 mg mL^{-1} gentamycin. Cultures were incubated at 37 °C, 3% O_2, 3% CO_2 and 94% N_2. Synchronization of parasites in culture to ring stages was carried out by repetitive treatment with 5% (m/v) sorbitol. Parasite growth and parasitemia were monitored by assessing Giemsa-stained blood smears under the microscope.

Drug treatment

Drug treatment experiments were conducted in 96-well plates with different concentrations of each drug in triplicate for each concentration. For this assay, 1% parasitemia and 2% hematocrit were set for each well and 200 μL of RPMI with 10% human serum and drug were added. The parasites were exposed to the drug and the 96-well plates were incubated for 48 h.

Flow cytometry analysis

Sample analysis was done according to an already published report.[11] In brief, after 48 h incubation, the plates were centrifuged at 3000 rpm for 5 min and the RPMI medium was removed. Any traces of drug were washed with phosphate buffered saline (PBS) solution (pH 7.2-7.4). The sample was incubated with 2% formaldehyde in PBS for 24 h to fix the parasite. After fixation, the samples were washed with PBS again. Permeabilization and staining was done with 0.1% Triton-X100 and 5 nM YOYO-1 dye (Molecular Probes).[15] This was done by incubating the sample reaction mixture at 37 °C for 30 min. Parasitemia

and proportions of parasites at each concentration of all drugs and control samples (without drug treatment) were determined from dot plots [side scatter (SSC) *vs.* fluorescence] of 10^5 cells acquired on a FACS Calibur flow cytometer using CELLQUEST software (Becton & Dickinson). YOYO-1 was excited with a 488 nm argon laser and fluorescence emission was collected at 520-530 nm. Parameters subject to adjustment of the FACS Calibur flow cytometer were forward scatter (FSC) (log scale, E-1), SSC (log scale, 269), FL-1 (log scale, 530), and compensation parameters were FL1 − 0.8% FL2 and FL2 − 23.6% FL1.[11]

Statistical analysis

GraphPad Prism (GraphPad Software) software was used for statistical analysis to calculate IC_{50} values. At least three independent experiments were performed for each experimental condition (Tables S1-S5).

Results and Discussion

(−)-Cassine **1** was isolated as an optically active, white solid, with m.p. 54.3 °C. Its molecular weight was measured by HRMS, and the molecular formula was established as $C_{18}H_{35}NO_2$, which inferred two degrees of unsaturation. The observed protonated molecular ion at *m/z* 298.2748 [M + H]$^+$ was close to the value calculated for $C_{18}H_{36}NO_2$, 298.2746. The IR absorption bands were assigned to hydroxy (3203 cm^{-1}) and carbonyl (1709 cm^{-1}) functionalities. Examination of the ^{1}H, ^{13}C, and DEPT NMR spectra recorded in chloroform-*d* (Table 1) showed the presence of a 2,3,6-trisubstituted piperidine ring. It was possible to observe a double quadruplet at δ 2.82 (1H, $J_{2,7}$ 6.5 and $J_{2,3}$ 1.0 Hz, H-2, δ_C 56.20), a broad singlet at δ 3.59 (1H, H-3, δ_C 68.04), two methylenes at δ 32.11 (2H, δ_H 1.91, H-4a and δ_H 1.51, H-4b), and δ 25.78 (2H, δ_H 1.50, H-5a and δ_H 1.40, H-5b), a multiplet at 2.59 (1H, H-4a, δ_C 57.60), and a methyl group at δ 1.16 (d, $J_{2,7}$ 6.5 Hz, H-7, δ_C 18.52). Additionally, ^{13}C NMR data evidenced ten methylenes at δ 36.71 (C-1', δ_H 1.50, H-1'a and δ_H 1.40, H-1'b), 25.99 (C-2', δ_H 1.30), 29.72 (C-3', δ_H 1.26), 29.64 (C-4', δ_H 1.26), 29.76 (C-5', δ_H 1.26), 29.60 (C-6', δ_H 1.26), 29.39 (C-7', δ_H 1.26), 29.95 (C-8', δ_H 1.26), 24.09 (C-9', δ_H 1.56), 44.04 (C-10', δ_H 2.41, t, *J* 7.0 Hz), a carbonyl at δ 209.63 (C-11'), and a methyl group at δ 30.07 (C-12, δ_H 2.13, s), which suggested the presence of a long linear side-chain, typical of the structural feature of piperidine alkaloids, as assembled for **1**. Furthermore, the side-chain (C-1'−C-12') attached at C-6 of the piperidine nucleus was also confirmed by an HMBC NMR experiment. Three-bond correlations were observed from H-5 to C-1', H-1' to C-5, and H-6 to C-1' and C-2' (Figure 2), supporting

a 2-methyl-3-hydroxy-6-*n*-alkyl piperidine substitution pattern. The methyl-ketone at the end of the straight side-chain (C-11') and the methyl group at C-2, were also defined by HMBC data analysis, for which the main correlations are represented in Figure 2. The relative configuration of C-2, C-3 and C-6, were established by spectroscopy, particularly from their hydrogen-hydrogen coupling constants and nuclear Overhauser effect spectroscopy (NOESY) 1D correlations observed when H-2 (δ 2.82) was irradiated to show correlations with H-3 (δ 3.59), H-4b (δ 1.51) and H-6 (δ 2.59) (Figure S34). Furthermore, polarimetric analysis ($[\alpha]_D^{25}$ −0.62) confirm the absolute stereochemistry which

was established by Rice and Coke.[13] The overall data analysis confirms the structure of the piperidine alkaloid **1** as (2*R*,3*R*,6*S*)-2-methyl-6-(11-oxododecyl)piperidin-3-ol, named (−)-cassine.

(−)-Spectaline **2** was also isolated as an optically active, white solid, with m.p. 67.7 °C. Its molecular weight was measured by HRMS, and the molecular formula was established as $C_{20}H_{39}NO_2$, which implied two degrees of unsaturation. The observed protonated molecular ion at *m/z* 326.3056 [M + H]$^+$ was close to the value calculated for $C_{20}H_{40}NO_2$, 326.3054. The IR absorption bands were assigned to hydroxy (3089 cm^{-1}), and carbonyl (1707 cm^{-1})

Table 1. NMR Spectroscopic data for **1** and **2** (δ in ppm)[a]

Position	**1** (chloroform-*d*)		**2** (methanol-*d*₄)	
	δ_C (mult.)	δ_H[b] (mult., *J* / Hz)	δ_C (mult.)	δ_H[b] (mult., *J* / Hz)
2	56.20 (CH)	2.82 dq (6.5; 1.0)	56.35 (CH)	2.78 dq (7.0; 1.5)
3	68.04 (CH)	3.59 br s	67.97 (CH)	3.59 br s
4a	32.11 (CH₂)	1.91 m	32.57 (CH₂)	1.90 m
4b		1.51 m		1.63 m
5a	25.78 (CH₂)	1.50 m	26.01 (CH₂)	1.52 m
5b		1.40 m		1.39 m
6	57.60 (CH)	2.59 m	57.79 (CH)	2.58 m
7	18.52 (CH₃)	1.16 d (6.5)	18.16 (CH₃)	1.12 d (7.0)
1'a	36.71 (CH₂)	1.50 m	37.34 (CH₂)	1.49 m
1'b		1.40 m		1.35 m
2'	25.99 (CH₂)	1.30 m	26.79 (CH₂)	1.36 m
3'	29.72[c] (CH₂)	1.26 br s	30.51[c] (CH₂)	1.29 br s
4'	29.64[c] (CH₂)	1.26 br s	30.61[c] (CH₂)	1.29 br s
5'	29.76[c] (CH₂)	1.26 br s	30.70[c] (CH₂)	1.29 br s
6'	29.60[c] (CH₂)	1.26 br s	30.67[c] (CH₂)	1.29 br s
7'	29.39[c] (CH₂)	1.26 br s	30.67[c] (CH₂)	1.29 br s
8'	29.95[c] (CH₂)	1.26 br s	30.58[c] (CH₂)	1.29 br s
9'	24.09 (CH₂)	1.56 m	30.24[c] (CH₂)	1.29 br s
10'	44.04 (CH₂)	2.41 t (7.0)	30.86[c] (CH₂)	1.29 br s
11'	209.63 (C)	–	24.89 (CH₂)	1.55 m
12'	30.07 (CH₃)	2.13 s	44.32 (CH₂)	2.46 t (7.0)
13'	–	–	212.21 (C)	–
14'	–	–	29.76 (CH₃)	2.12 s

[a]Recorded at 500 and 125 MHz for ^{1}H and ^{13}C NMR, respectively; [b]multiplicity of signals is given as follows: s, singlet; br, broad; d, doublet; t, triplet; dq, double quadruplet; m, multiplet; [c]the assignments were based on calculated δ_C (ChemDraw Ultra 10.0) and may be interchanged in the column.
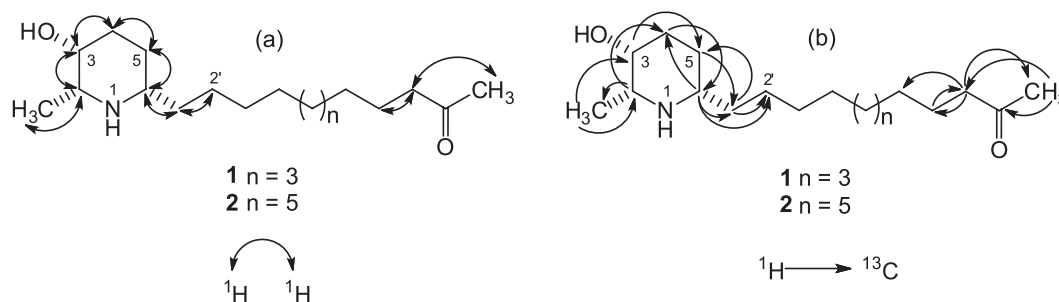
Figure 2. Key COSY (a) and HMBC (b) correlations for compounds **1** and **2**.

functional groups. Analysis of the 1D and 2D NMR data collected for **2** (Table 1; Figure 2) confirmed the same substitution pattern for **1**, except for two more methylene groups on the straight side-chain at C-6. Therefore, it had the same stereochemistry and structural features of **1** which was (2*R*,3*R*,6*S*)-2-methyl-6-(13-oxotetradecyl)piperidin-3-ol (Figure S57).

The two natural products and semisynthetic derivatives were assessed for their antimalarial inhibitory activity using flow cytometry test. Among them, **1** (IC$_{50}$ 1.82 μM) and **2** (IC$_{50}$ 2.76 μM) were more effective (IC$_{50}$ < 5.00 μM) than **3** (IC$_{50}$ 24.47 μM) and **4** (IC$_{50}$ 25.14 μM) in comparison with the standard compound chloroquine (IC$_{50}$ 0.30 μM) (Figures 3-7), which led us to deduce a moderate activity against *P. falciparum* 3D7 strain for the tested alkaloids (**1** and **2**). Some evidence on the structural features of these compounds, as the size of the straight side-chain combined with the values found for inhibitory concentration showed that the compounds with shorter side-chain (**1** and **3**) were more effective against *P. falciparum*, in comparison with the homologous (**2** and **4**). Additionally, the acetyl group in the parent structures at 3-*O* positions (**3** and **4**) reduced the antimalarial effectivity of the alkaloids. These findings

were in agreement with a biological criterion established by Nwaka *et al.*[16] to screening for hit-to-lead compounds as antimalarial agents. According to the author, all compounds with an in vitro IC$_{50}$ ranging from 1 to 10 μM can be classified as a 'hit'. These findings suggest **1** and **2** as examples of hits, and thus are potential candidates for further investigations aiming natural antimalarial drugs. To reinforce this statement a recent work reported piperidine alkaloids as antimalarial agents.[17] Furthermore, the
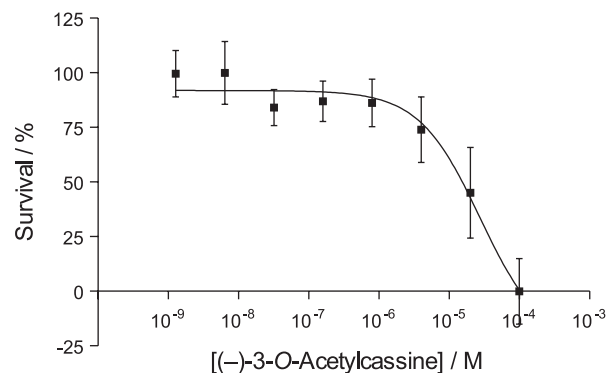
Figure 5. IC$_{50}$ value of (−)-3-*O*-acetylcassine (**3**) against *P. falciparum* was calculated to be 24.47 μM.

Figure 3. IC$_{50}$ value of (−)-cassine (**1**) against *P. falciparum* was calculated to be 1.82 μM.
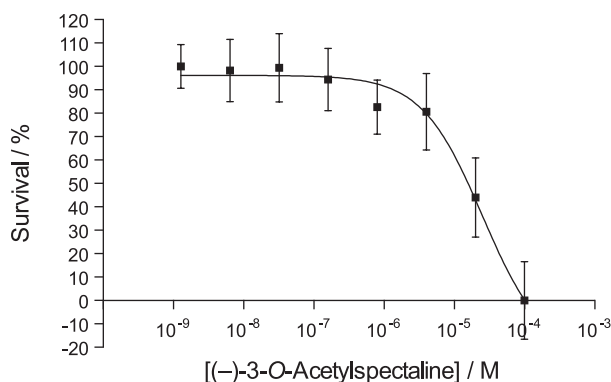
Figure 6. IC$_{50}$ value of (−)-3-*O*-acetylspectaline (**4**) against *P. falciparum* was calculated to be 25.14 μM.

Figure 4. IC$_{50}$ value of (−)-spectaline (**2**) against *P. falciparum* was calculated to be 2.76 μM.
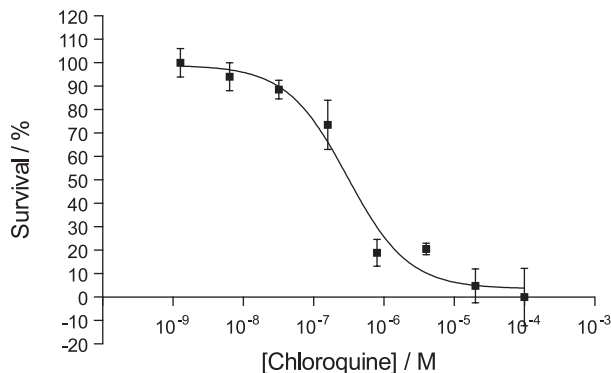
Figure 7. IC$_{50}$ value of chloroquine (positive control) against *P. falciparum* was calculated to be 0.30 μM.

alkaloids described here show a novel structural scaffold when compared to other natural products clinically used, like quinine or artemisinin and their derivatives, oppening a new window for further studies on drug discovery and lead optimization for innovative antimalarial medicines.

Conclusions

Nowadays, malaria remains one of the most widespread infectious diseases causing thousands of deaths around the world and one of the major problems is the growing parasite resistance to current antimalarial drugs. This study reports the antimalarial activity of two piperidine alkaloids (**1** and **2**) isolated from *Senna spectabilis* and two semisynthetic derivatives (**3** and **4**). The natural compound with shorter side chain (**1**) is more effective against *P. falciparum*. Addition of acetyl group to the parent structures at 3-*O* positions (**3** and **4**) reduced the antimalarial effectivity of alkaloids. According to these data, the alkaloids were chemical hits and potential candidates for further investigations.

Supplementary Information

Supplementary data (Figures S1-S61, Tables S1-S5), including TLC plates as well as DSC analysis, IR, high-resolution mass, ^{1}H and ^{13}C NMR and selected 2D spectra for compounds **1** to **4**, are available free of charge at http://jbcs.sbq.org.br as a PDF file.

Acknowledgments

References

1. Hall, B. F.; Fauci, A. S.; *J. Infect. Dis.* **2009**, *200*, 1639; World Health Organization; *Global Report on Antimalarial Drug Efficacy and Drug Resistance: 2000-2010*; WHO Press: Geneva, 2010. Available at http://www.who.int/malaria/publications/atoz/9789241500470/en/ accessed in August 2014.

2. Nayyar, G. M. L.; Breman, J. G.; Newton, P. N.; Herrington, J.; *Lancet Infect. Dis.* **2012**, *12*, 488.

3. Cammack, N.; *Science* **2011**, *333*, 705.

4. Valecha, N.; Joshi, H.; Mallick, P. K.; Sharma, S. K.; Kumar, A.; Tyagi, P. K.; Shahi, B.; Das, M. K.; Nagpal, B. N.; Dash, A. P.; *Acta Trop.* **2009**, *111*, 21.

5. Bolzani, V. S.; Valli, M.; Pivatto, M.; Viegas Jr., C.; *Pure Appl. Chem.* **2012**, *84*, 1837.

6. Viegas Jr., C.; Bolzani, V. S.; Furlan, M.; Barreiro, E. J.; Young, M. C. M.; Tomazela, D.; Eberlin, M. N.; *J. Nat. Prod.* **2004**, *67*, 908.

7. Pivatto, M.; Crotti, A. E. M.; Lopes, N. P.; Castro-Gamboa, I.; Rezende, A.; Viegas Jr., C.; Young, M. C. M.; Furlan, M.; Bolzani, V. S.; *J. Braz. Chem. Soc.* **2005**, *16*, 1431.

8. Viegas Jr., C.; Bolzani, V. S.; Pimentel, L. S.; Castro, N. G.; Cabral, R. F.; Costa, R. S.; Floyd, C.; Rocha, M. S.; Young, M. C.; Barreiro, E. J.; Fraga, C. A. M.; *Bioorg. Med. Chem.* **2005**, *13*, 4184.

9. Viegas Jr., C.; Silva, D. H. S.; Pivatto, M.; Rezende, A.; Castro-Gamboa, I.; Bolzani, V. S.; Nair, M. G.; *J. Nat. Prod.* **2007**, *70*, 2026.

10. Danuello, A.; Romeiro, N. C.; Giesel, G. M.; Pivatto, M.; Viegas Jr., C.; Verli, H.; Barreiro, E. J.; Fraga, C. A. M.; Castro, N. G.; Bolzani, V. S.; *J. Braz. Chem. Soc.* **2012**, *23*, 163.

11. Schuck, D. C.; Ribeiro, R. Y.; Nery, A. A.; Ulrich, H.; Garcia, C. R. S.; *Cytometry, Part A* **2011**, *79A*, 959.

12. Wagner, H.; Bladt, S.; *Plant Drug Analysis: A Thin Layer Chromatography Atlas*, 2ⁿᵈ ed.; Springer: Berlin, 2001; Touchstone, J. C.; Dobbins, M. F.; *Practice of Thin Layer Chromatography*, 2ⁿᵈ ed.; Wiley Interscience: New York, 1978.

13. Lythgoe, D.; Vernengo, M. J.; *Tetrahedron Lett.* **1967**, *12*, 1133; Highet, R. J.; *J. Org. Chem.* **1964**, *29*, 471; Rice Jr., W. Y.; Coke, J. L.; *J. Org. Chem.* **1966**, *31*, 1010; Christofidis, I.; Welter, A.; Jadot, J.; *Tetrahedron* **1977**, *33*, 977; Christofidis, I.; Welter, A.; Jadot, J.; *Tetrahedron* **1977**, *33*, 3005; Bolzani, V. S.; Gunatilaka, A. A. L.; Kingston, D. G. I.; *Tetrahedron* **1995**, *51*, 5929.

14. Lambros, C.; Vanderberg, J. P.; *J. Parasitol.* **1979**, *65*, 418.

15. Li, Q.; Gerena, L.; Xie, L.; Zhang, J.; Kyle, D.; Milhous, W.; *Cytometry, Part A* **2007**, *71A*, 297.

16. Nwaka, S.; Ramirez, B.; Brun, R.; Maes, L.; Douglas, F.; Ridley, R.; *PLoS Neglected Trop. Dis.* **2009**, *3*, e440.

17. Taniguchi, T.; Ogasawara, K.; *Org. Lett.* **2000**, *2*, 3193.

Supplementary Information

Antimalarial Activity of Piperidine Alkaloids from *Senna spectabilis* and Semisynthetic Derivatives

Marcos Pivatto,[*,a] *Luciene R. Baccini,*[b] *Abhinay Sharma,*[c] *Myna Nakabashi,*[c]
Amanda Danuello,[d] *Claudio Viegas Júnior,*[b] *Celia R. S. Garcia*[*,c] *and*
Vanderlan S. Bolzani[*,b]

[a]*Instituto de Química, Universidade Federal de Uberlândia, 38400-902 Uberlândia-MG, Brazil*

[b]*Núcleo de Bioensaios, Biossíntese e Ecofisiologia de Produtos Naturais (NuBBE),
Departamento de Química Orgânica, Instituto de Química, Universidade Estadual Paulista,
P.O. Box 355, 14801-970 Araraquara-SP, Brazil*

[c]*Departamento de Fisiologia, Instituto de Biociências, Universidade de São Paulo,
05508-900 São Paulo-SP, Brazil*

[d]*Departamento de Química, Instituto de Ciências Exatas, Naturais e Educação,
Universidade Federal do Triângulo Mineiro, 38064-200 Uberaba-MG, Brazil*

Figure S1. Thin-layer chromatography (TLC, SiO_2) of fractions from column chromatography (CC) of alkaloidal CH_2Cl_2 extract developed with $CHCl_3$-MeOH-NH_4OH (9:1:0.25) and revealed with iodochloroplatinate reagent.

*e-mail: pivatto@iqufu.ufu.br, cgarcia@usp.br, bolzaniv@iq.unesp.br
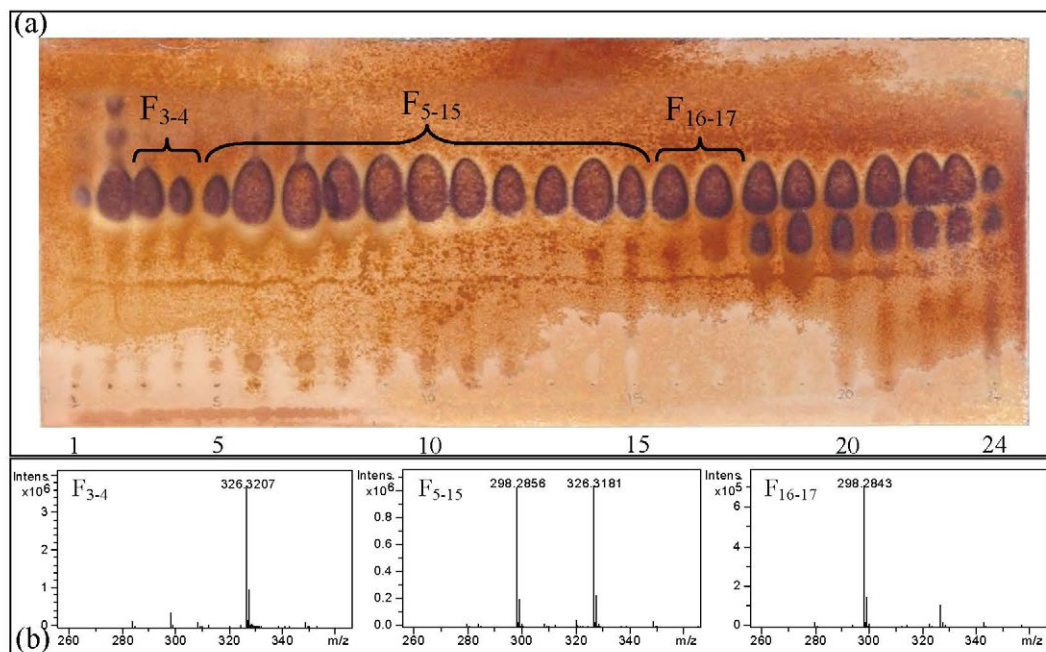
Figure S2. (a) TLC (SiO$_2$) of fractions from CC of F$_{1-4}$ developed with CHCl$_3$-MeOH-NH$_4$OH (9:1:0.25) and revealed with iodochloroplatinate reagent. (b) ESI-MS of F$_{3-4}$, F$_{5-15}$ and F$_{16-17}$.
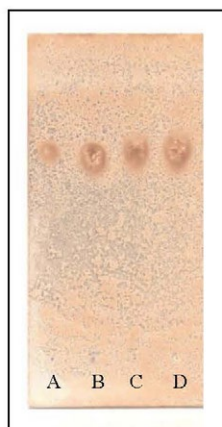
Figure S3. TLC (SiO$_2$) of **1** (A: free base, B: hydrochloride) and **2** (C: free base, D: hydrochloride) developed with CHCl$_3$-MeOH-NH$_4$OH (9:1:0.25) and revealed with iodochloroplatinate reagent.
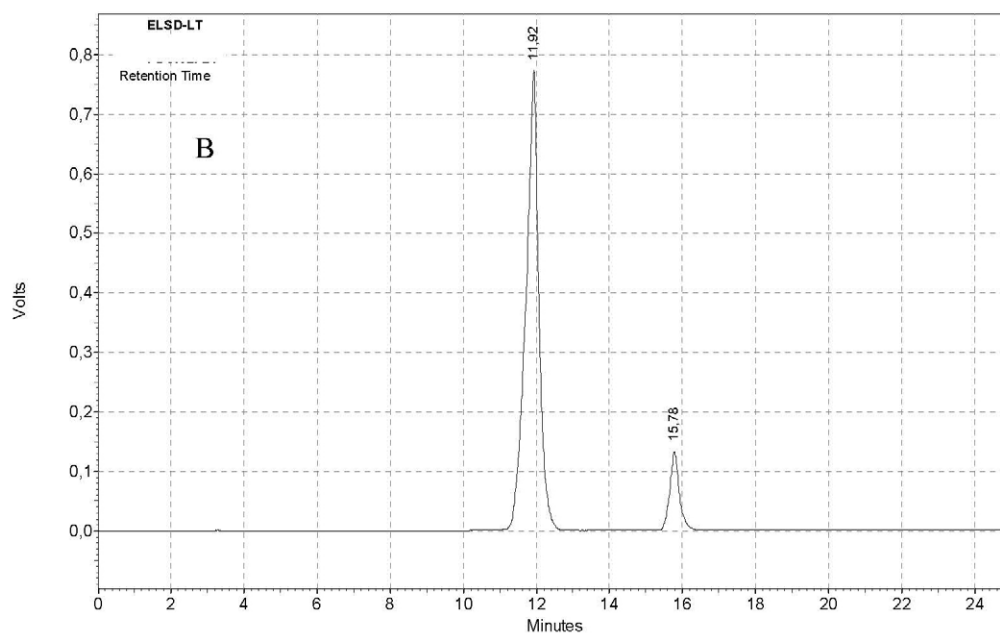
Figure S4. Analytical HPLC chromatogram on RP-C$_{18}$ of a mixture of **1** and **2** (F$_{5-15}$) eluted with a gradient of increasing MeOH in 0.1% HOAc aqueous solution (35-100, flow rate 8.0 mL min^{-1}, 25 min) and light scattering detector.
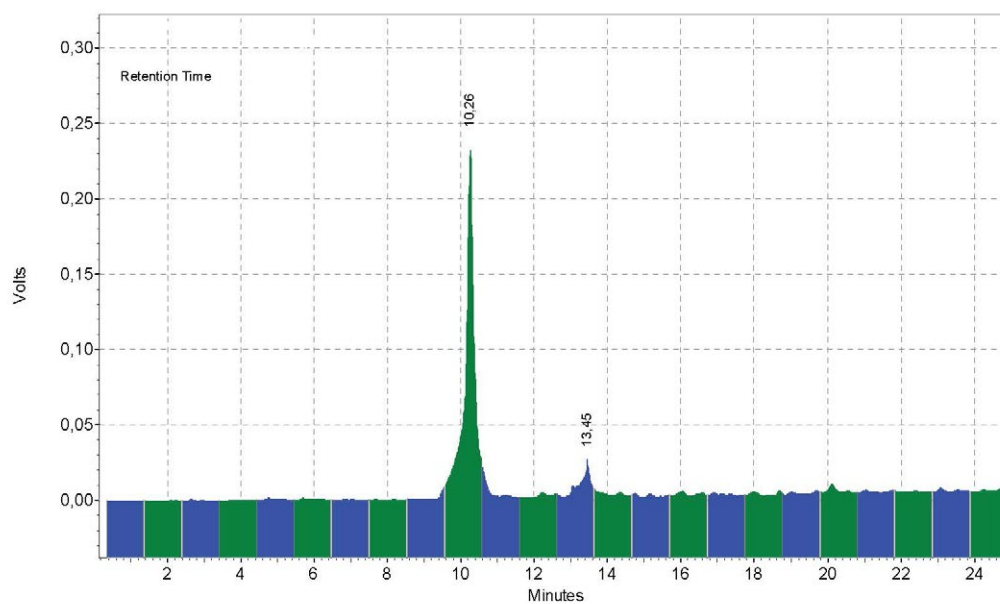
Figure S5. Preparative HPLC chromatogram on RP-C$_{18}$ of a mixture of **1** and **2** (F$_{5-15}$) eluted with a gradient of increasing MeOH in 0.1% HOAc aqueous solution (35-100, flow rate 8.0 mL min^{-1}, 25 min) and 284 nm UV detector.
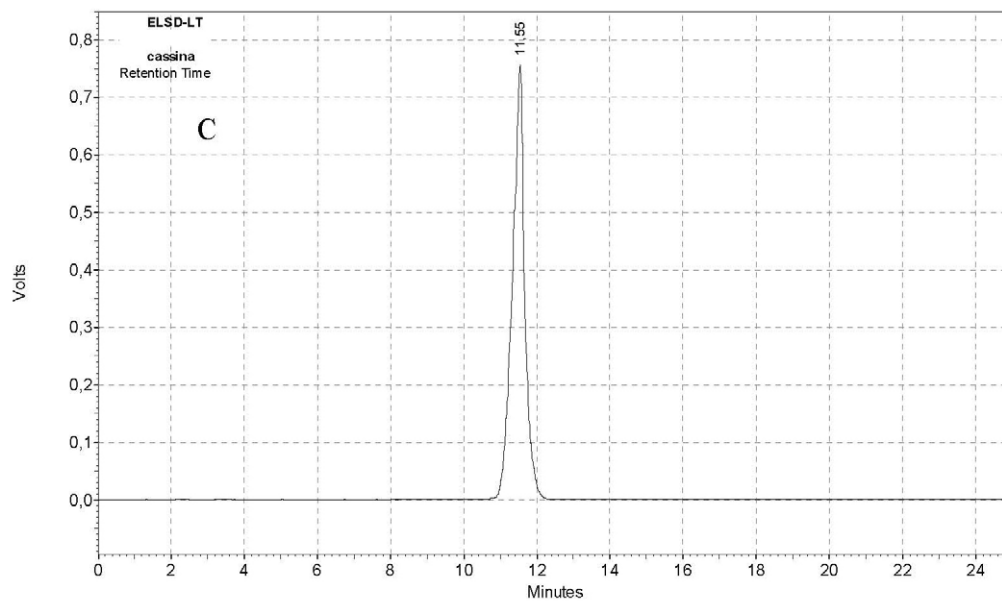
Figure S6. Analytical HPLC chromatogram on RP-C$_{18}$ of **1** (F$_{16-17}$) eluted with a gradient of increasing MeOH in 0.1% HOAc aqueous solution (35-100, flow rate 8.0 mL min^{-1}, 25 min) and light scattering detector.
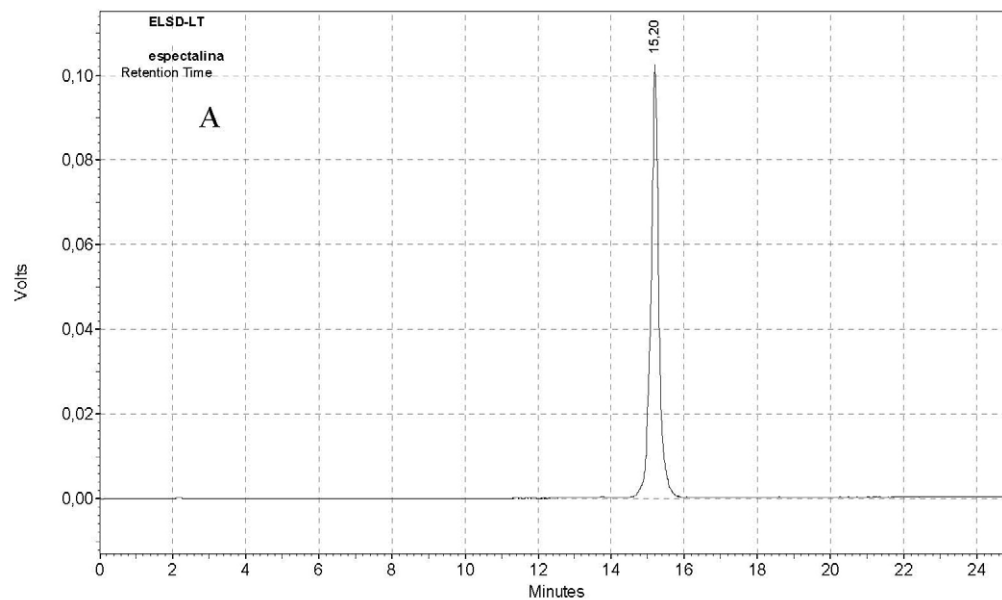
Figure S7. Analytical HPLC chromatogram on RP-C$_{18}$ of **2** (F$_{3-4}$) eluted with a gradient of increasing MeOH in 0.1% HOAc aqueous solution (35-100, flow rate 8.0 mL min^{-1}, 25 min) and light scattering detector.
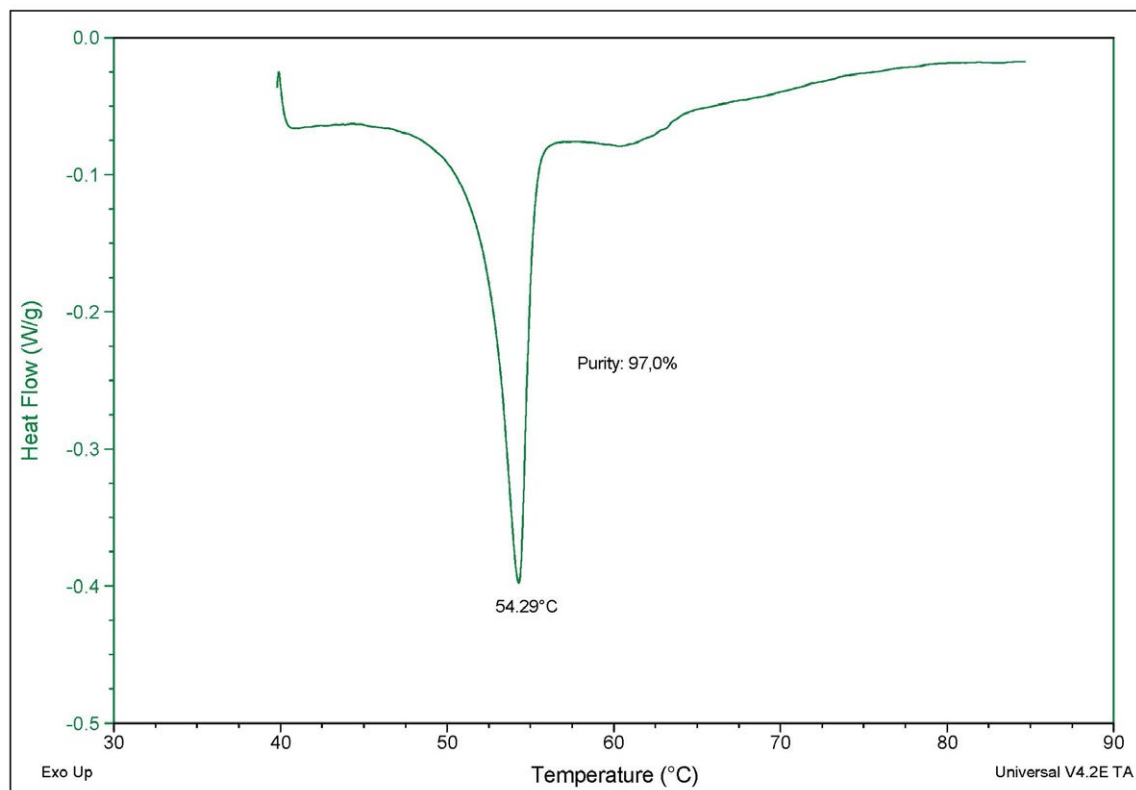
Figure S8. DSC analysis of **1**.
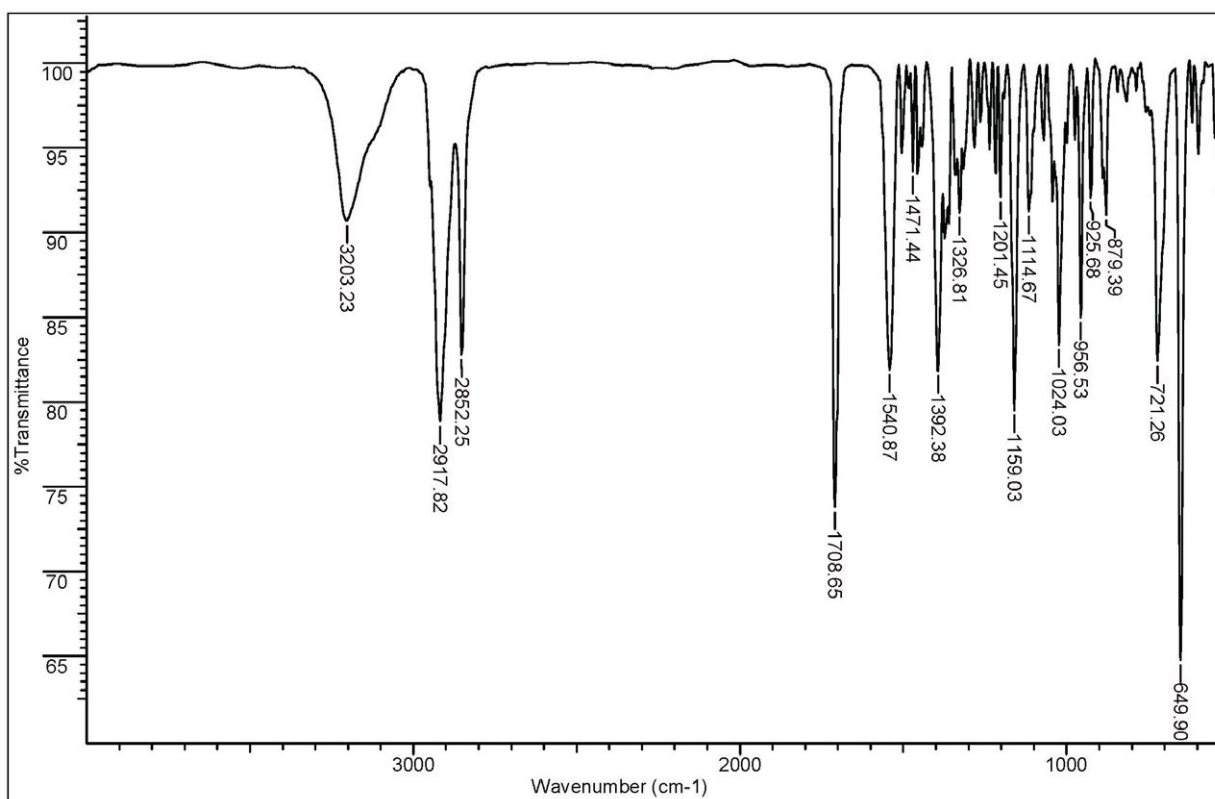
Figure S9. IR spectrum (film) of **1**.
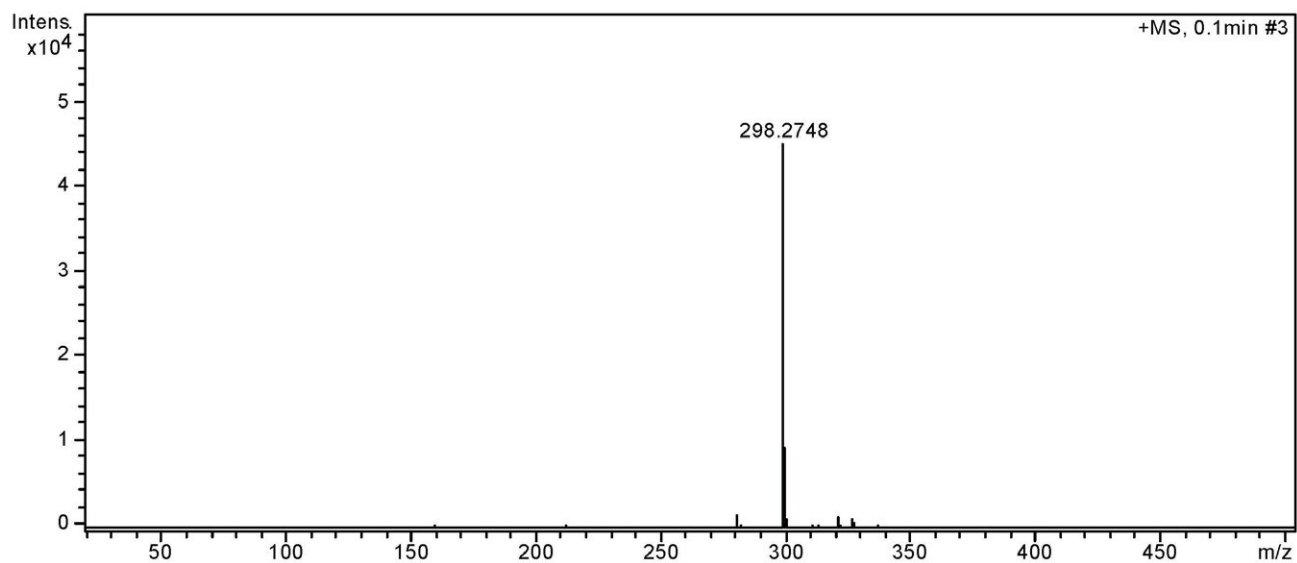
Figure S10. ESI-MS of **1** (HRMS *m/z* 298.2748 [M + H]$^+$ (calcd for $C_{18}H_{36}NO_2$: 298.2746)).
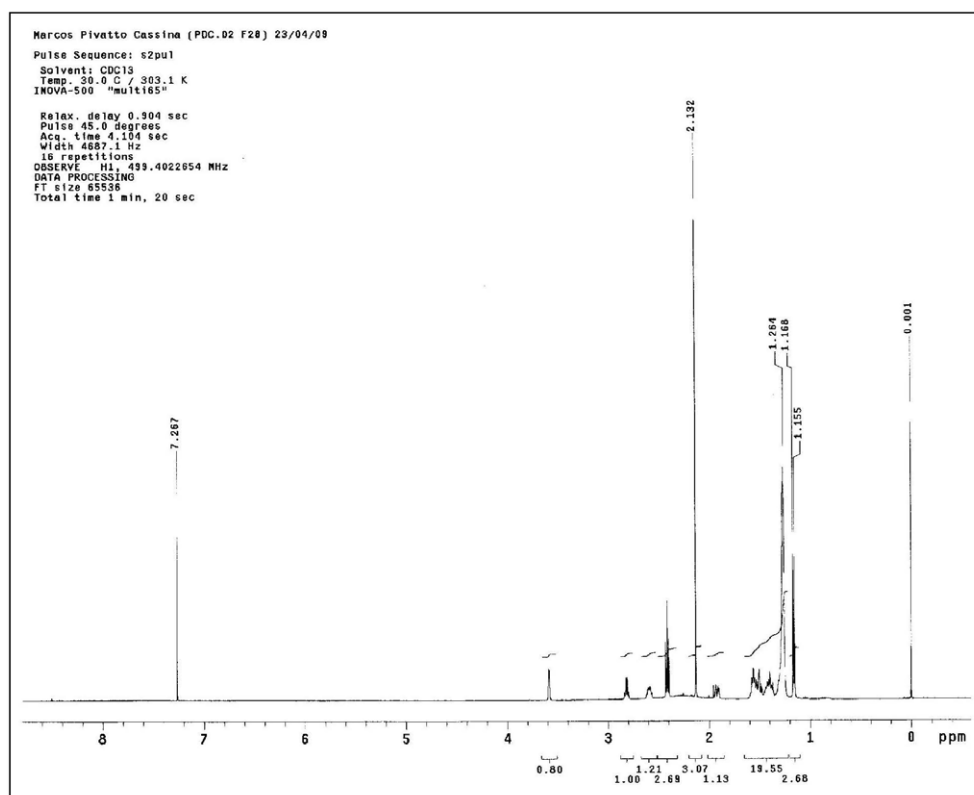
Figure S11. 500 MHz ^{1}H NMR spectrum of **1** in chloroform-*d*.
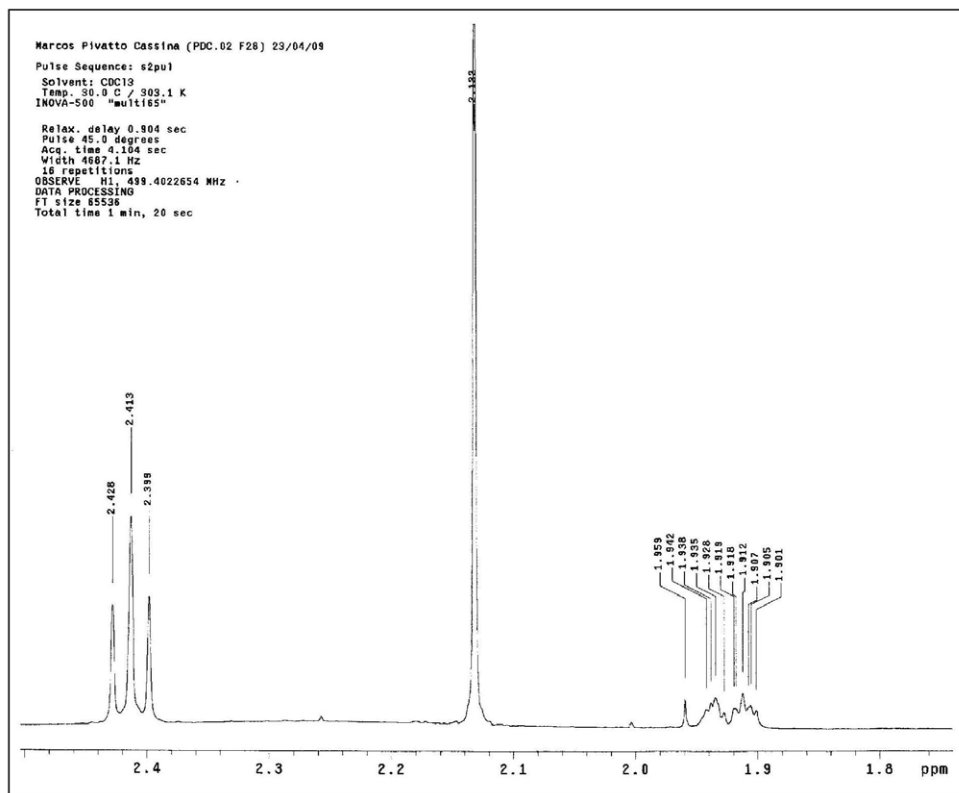
Figure S12. 500 MHz ¹H NMR spectrum (expansion δ 1.8-2.4) of **1** in chloroform-*d*.
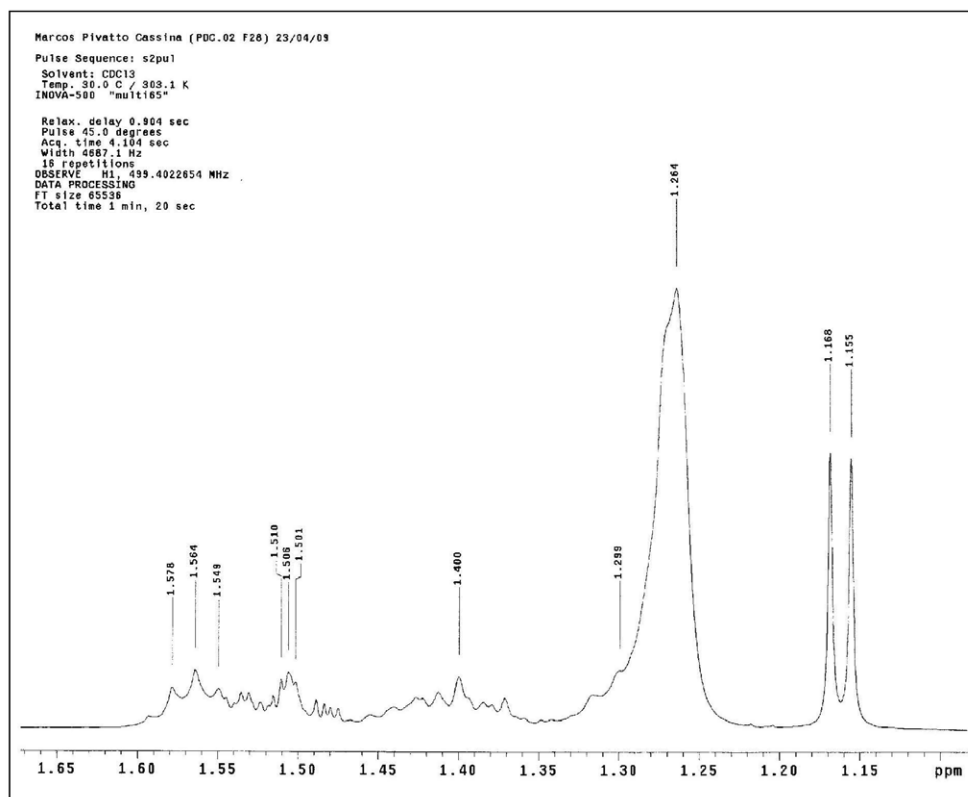
Figure S13. 500 MHz ¹H NMR spectrum (expansion δ 1.15-1.65) of **1** in chloroform-*d*.
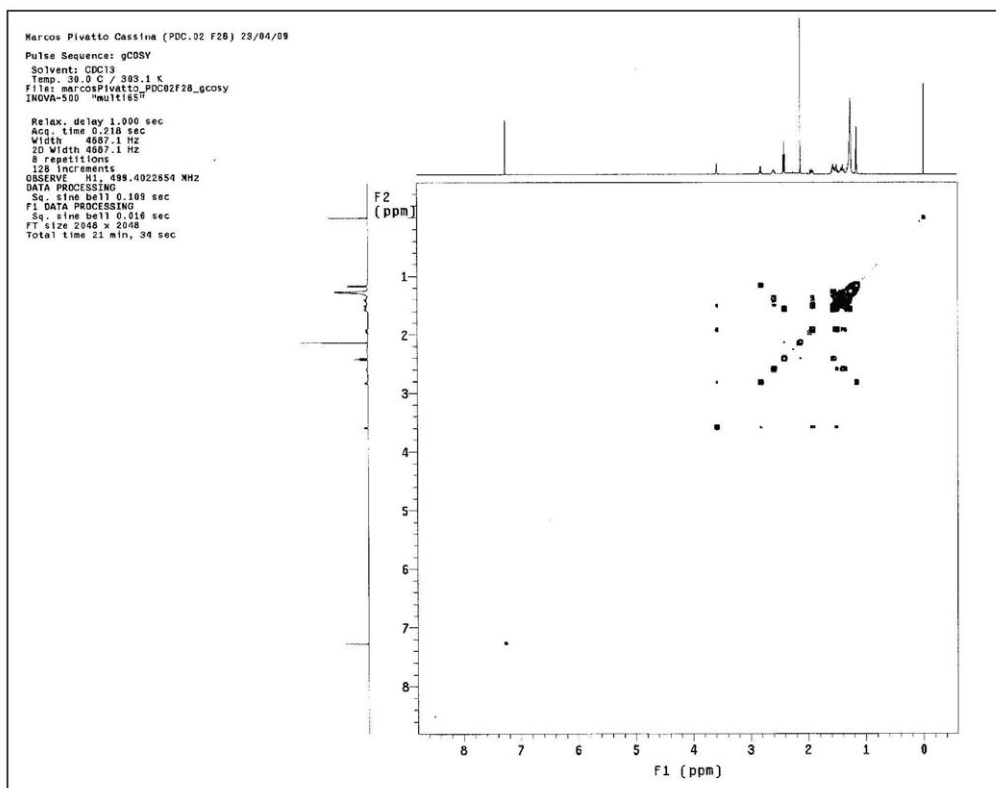
Figure S14. COSY spectrum of **1** in chloroform-*d*.
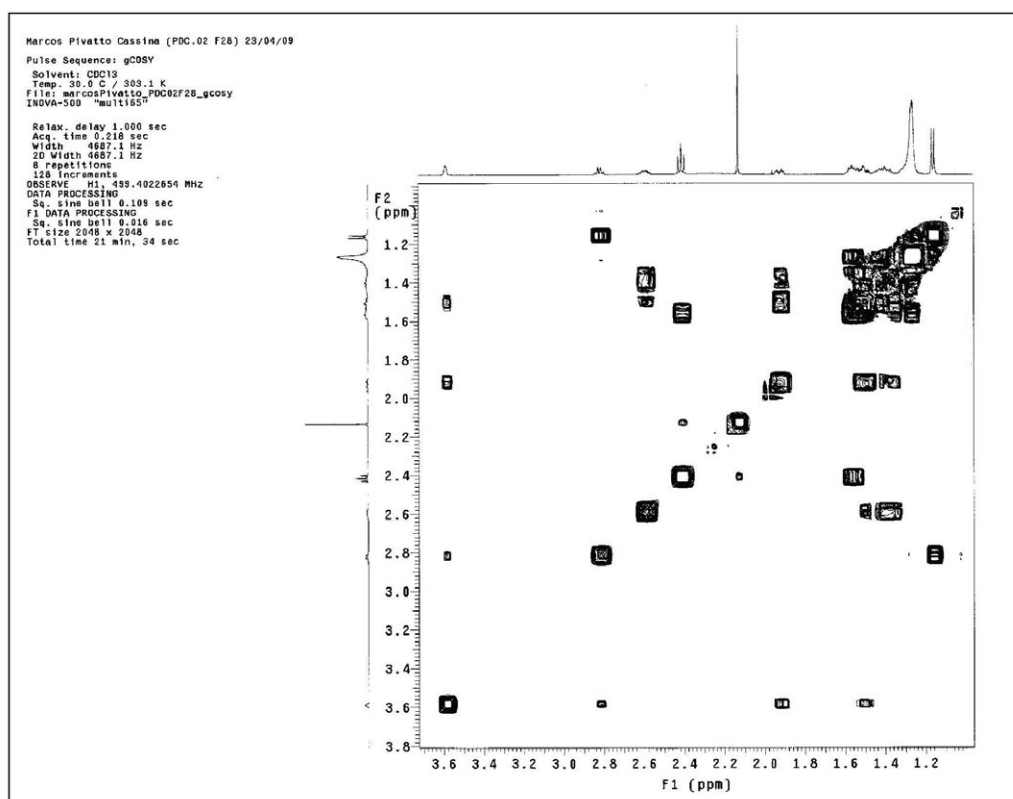
Figure S15. COSY spectrum (expansion δ 1.2-3.6) of **1** in chloroform-*d*.
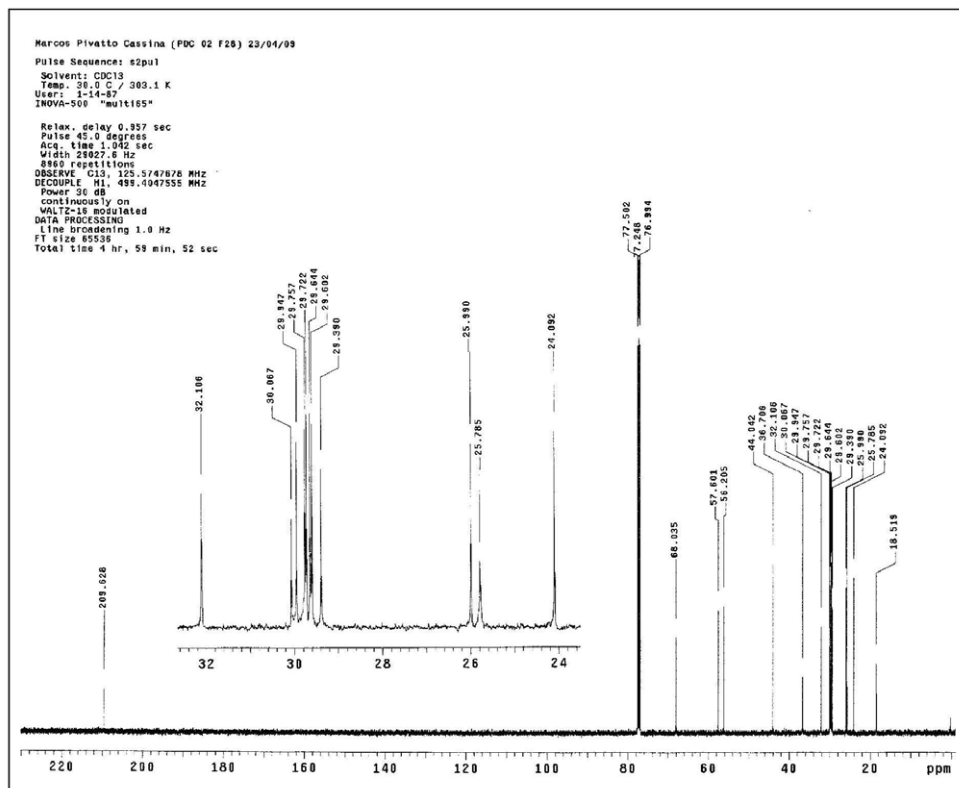
Figure S16. 125 MHz ^{13}C NMR spectrum of **1** in chloroform-*d*.
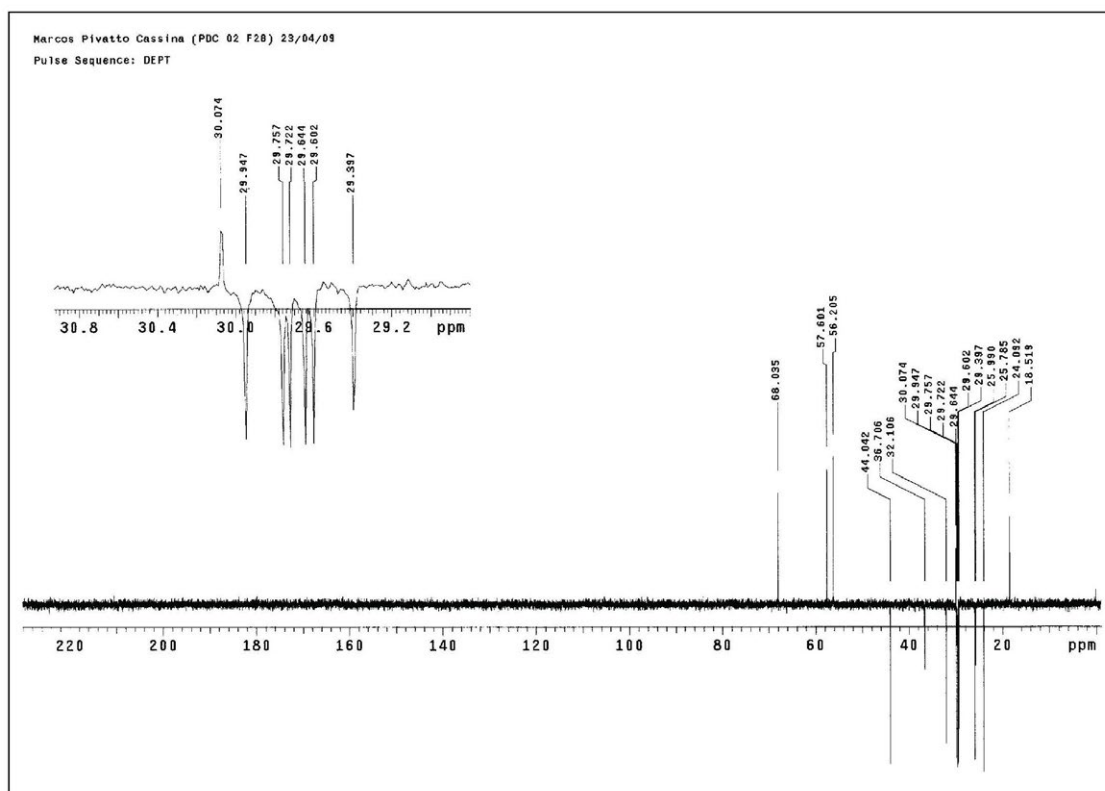
Figure S17. 125 MHz DEPT 135 NMR spectrum of **1** in chloroform-*d*.
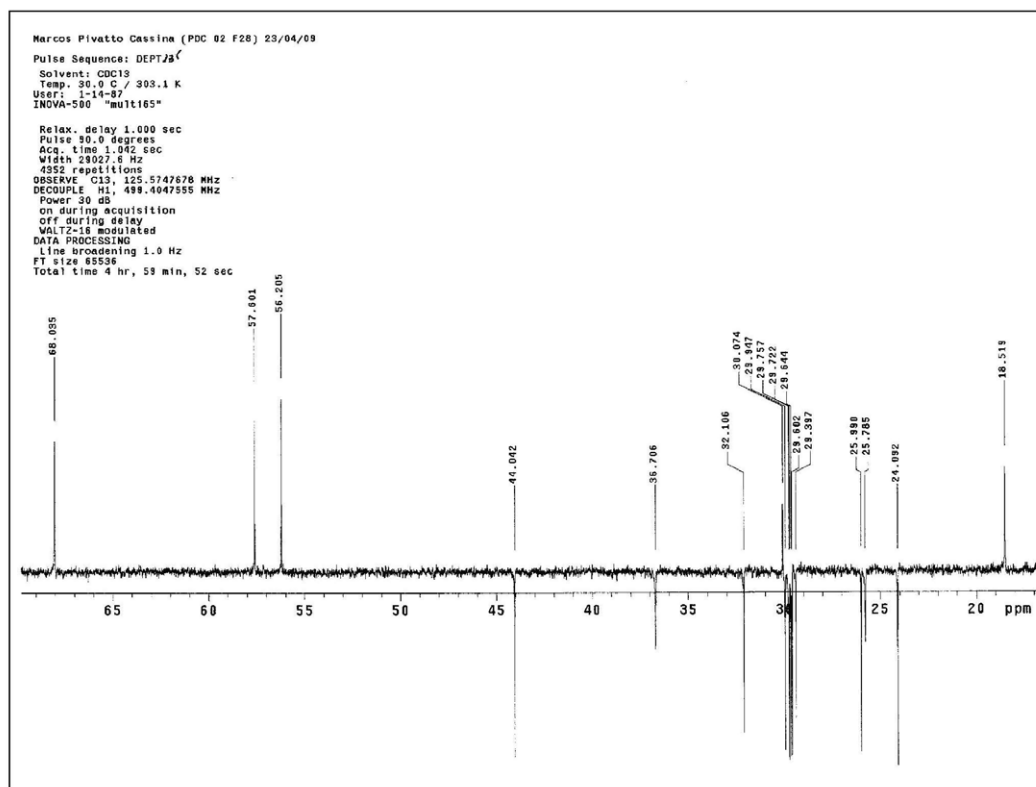
Figure S18. 125 MHz DEPT 135 NMR spectrum (expansion δ 20-65) of **1** in chloroform-*d*.
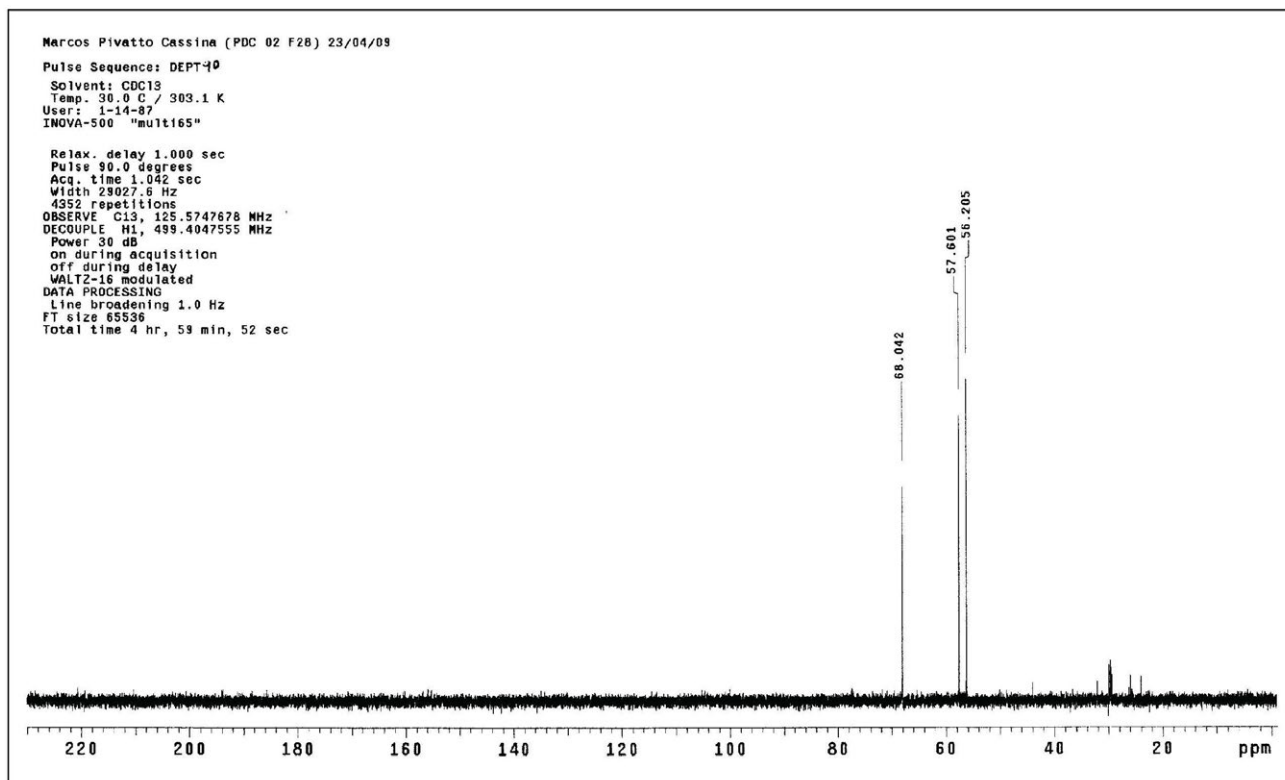
Figure S19. 125 MHz DEPT 90 NMR spectrum of **1** in chloroform-*d*.
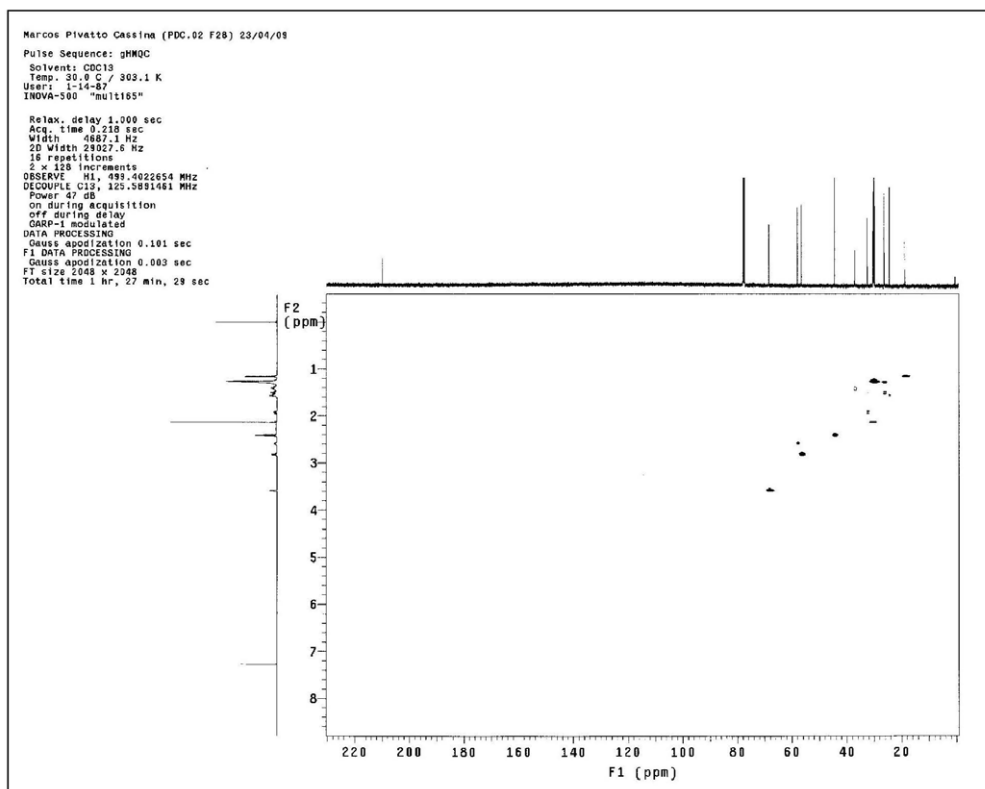
Figure S20. HMQC spectrum of **1** in chloroform-*d*.
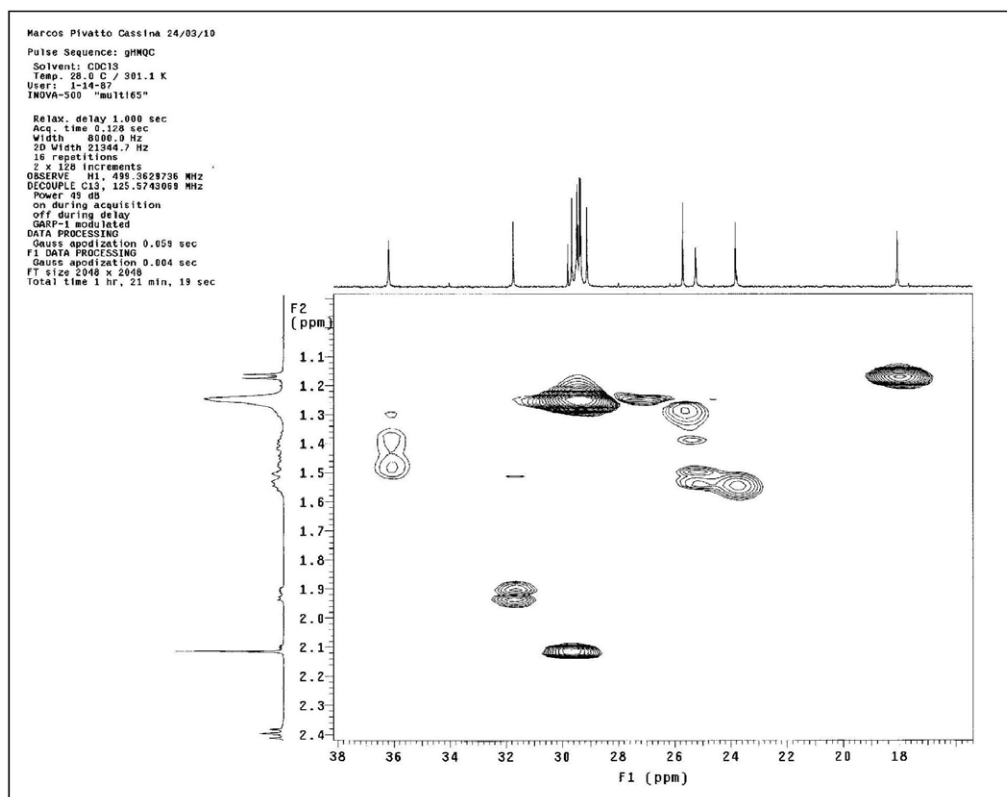
Figure S21. HMQC spectrum (expansion *δ* 18-38) of **1** in chloroform-*d*.
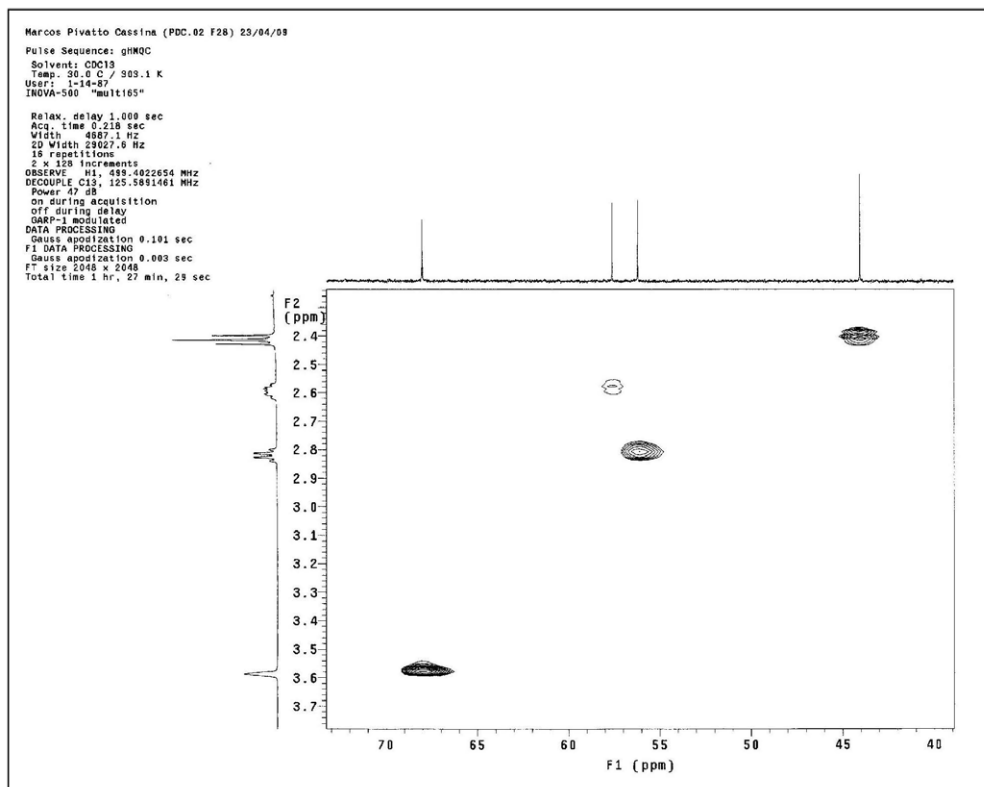
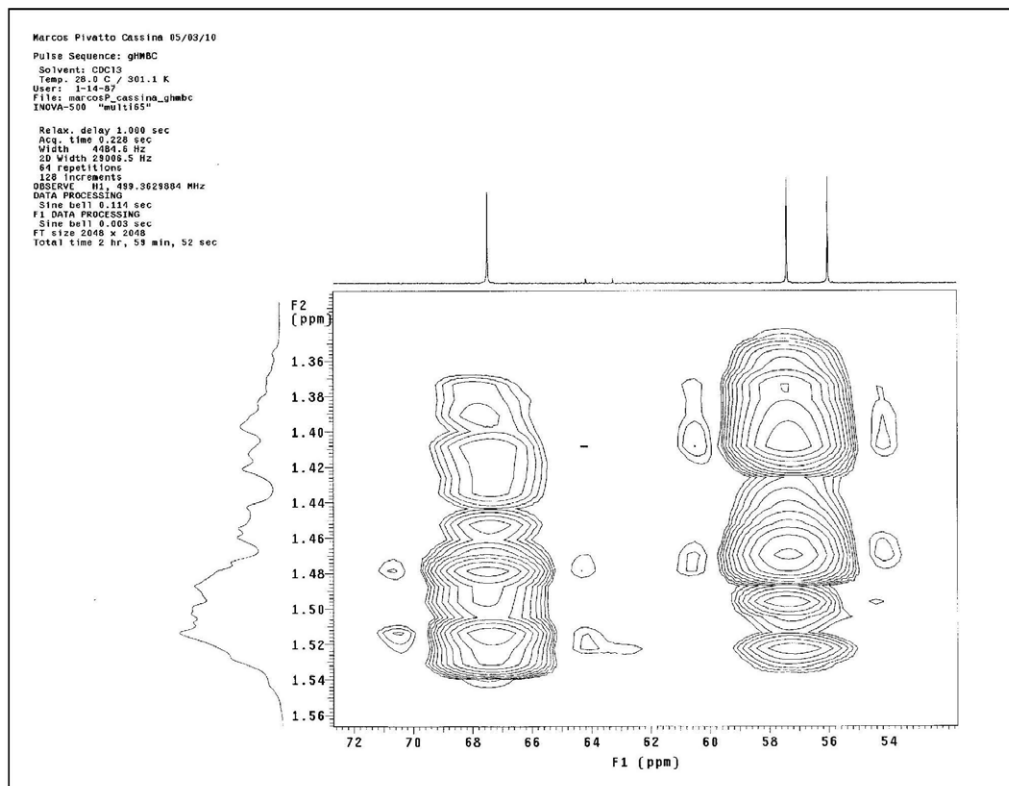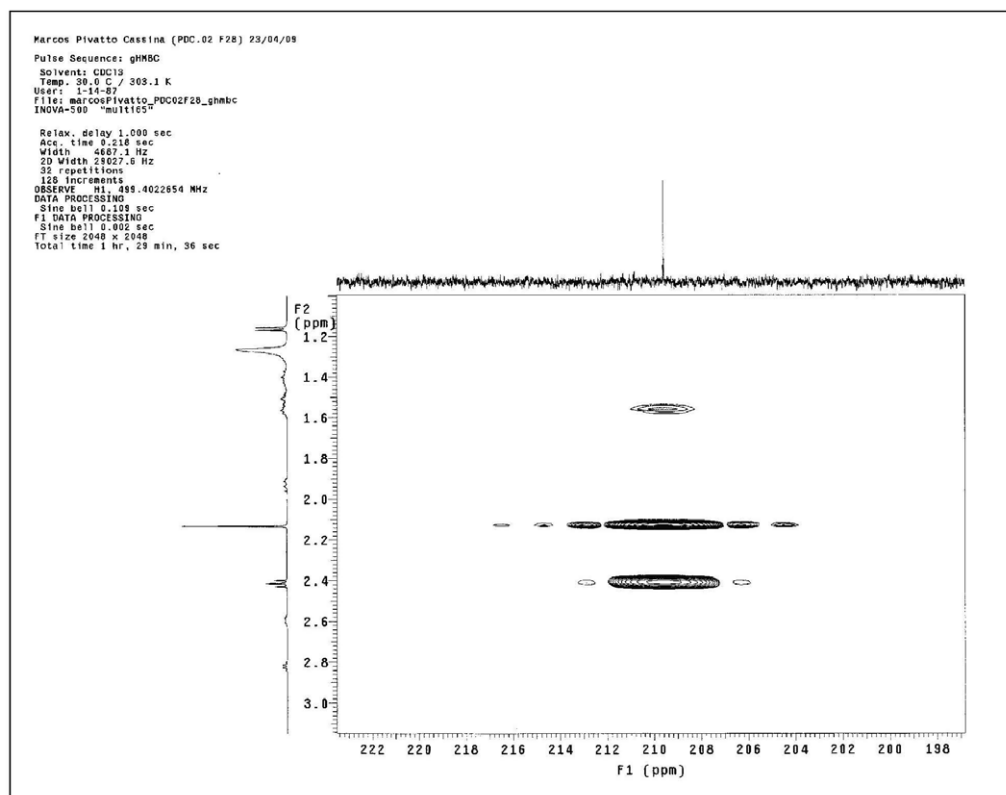**Figure S22.** HMQC spectrum (expansion δ 40-70) of **1** in chloroform-*d*.
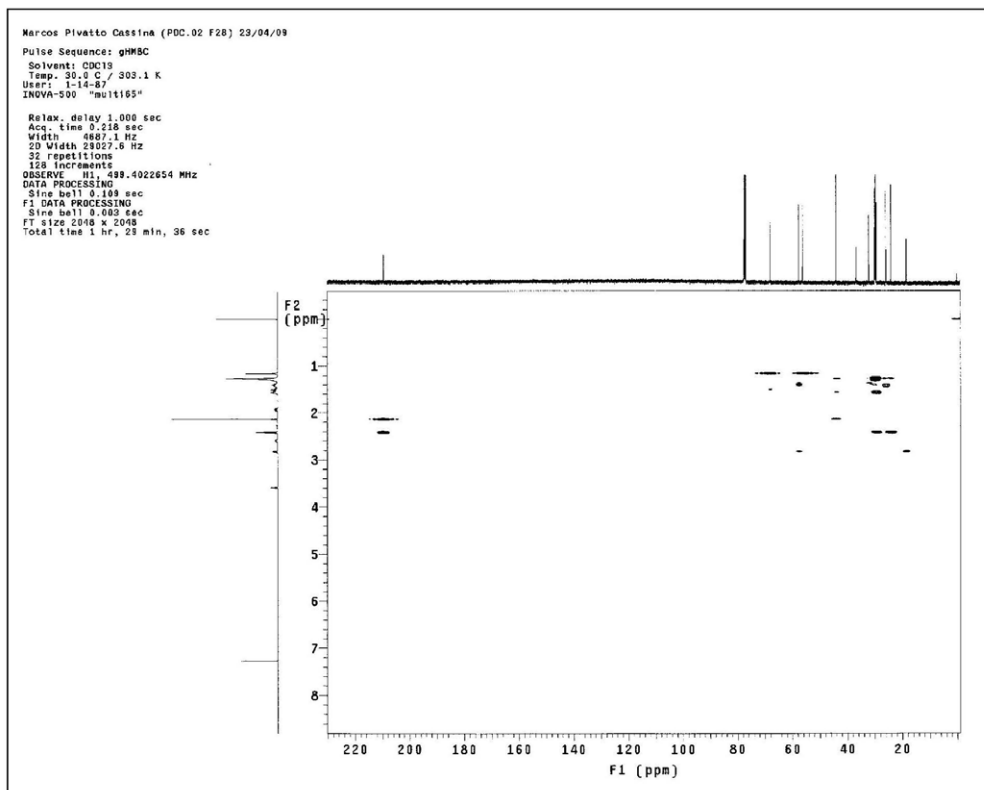
Figure S23. HMBC spectrum of **1** in chloroform-*d*.
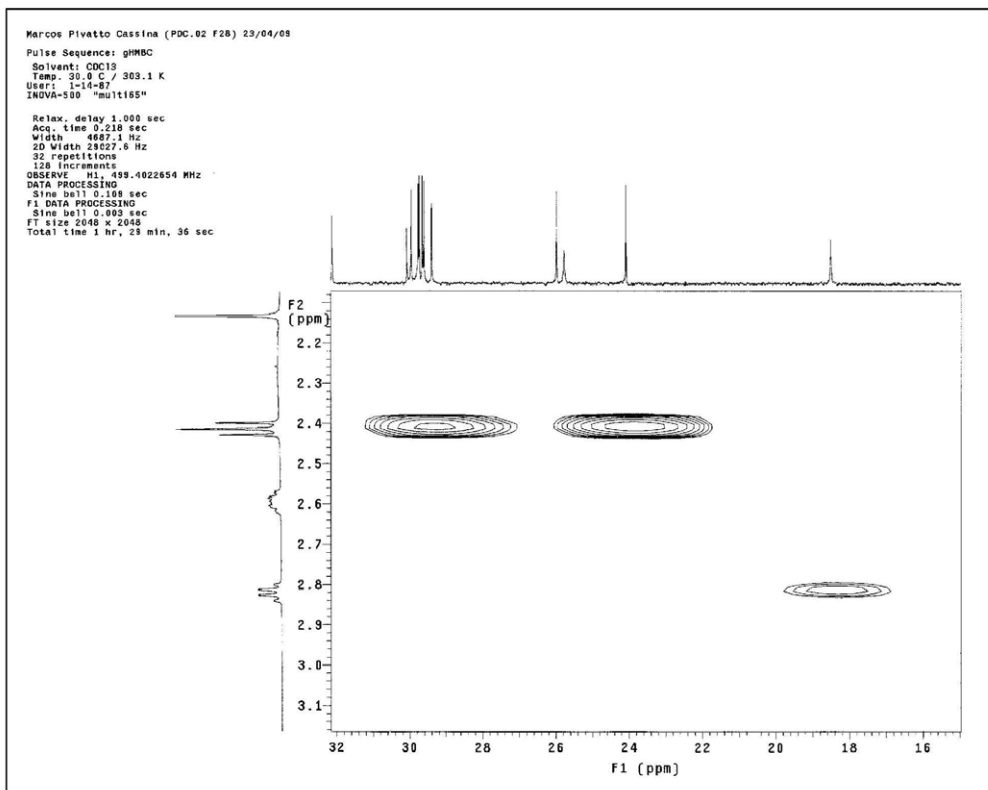
Figure S24. HMBC spectrum (expansion δ 16-32) of **1** in chloroform-*d*.
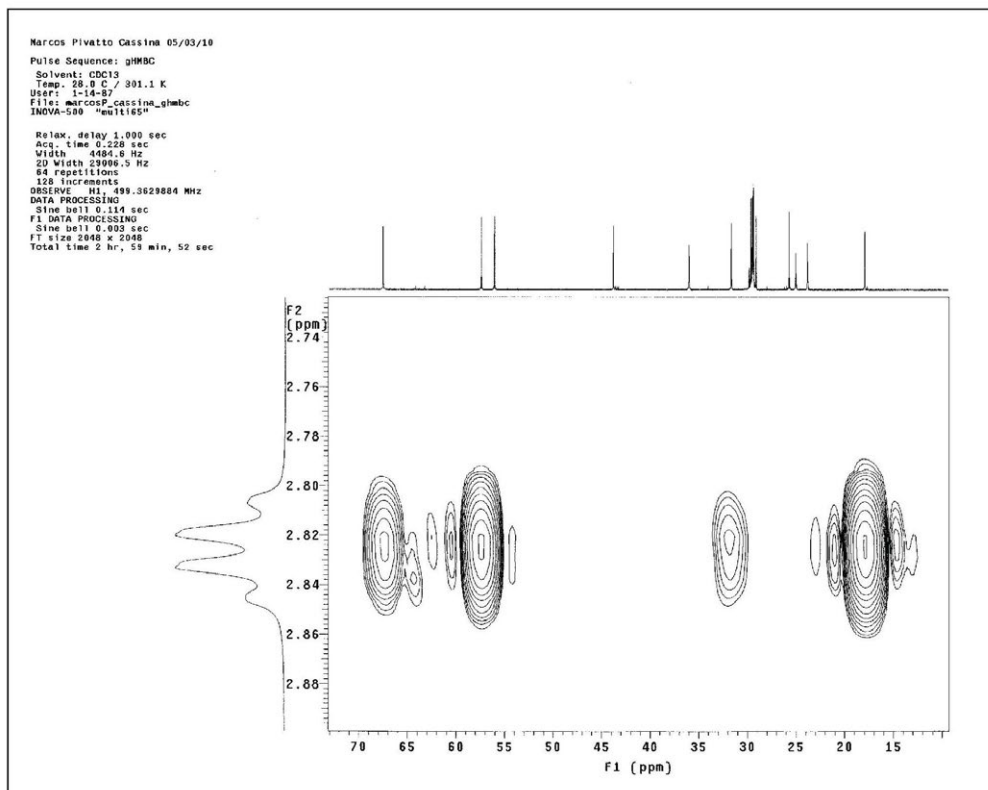
Figure S25. HMBC spectrum (expansion δ 15-70) of **1** in chloroform-*d*.
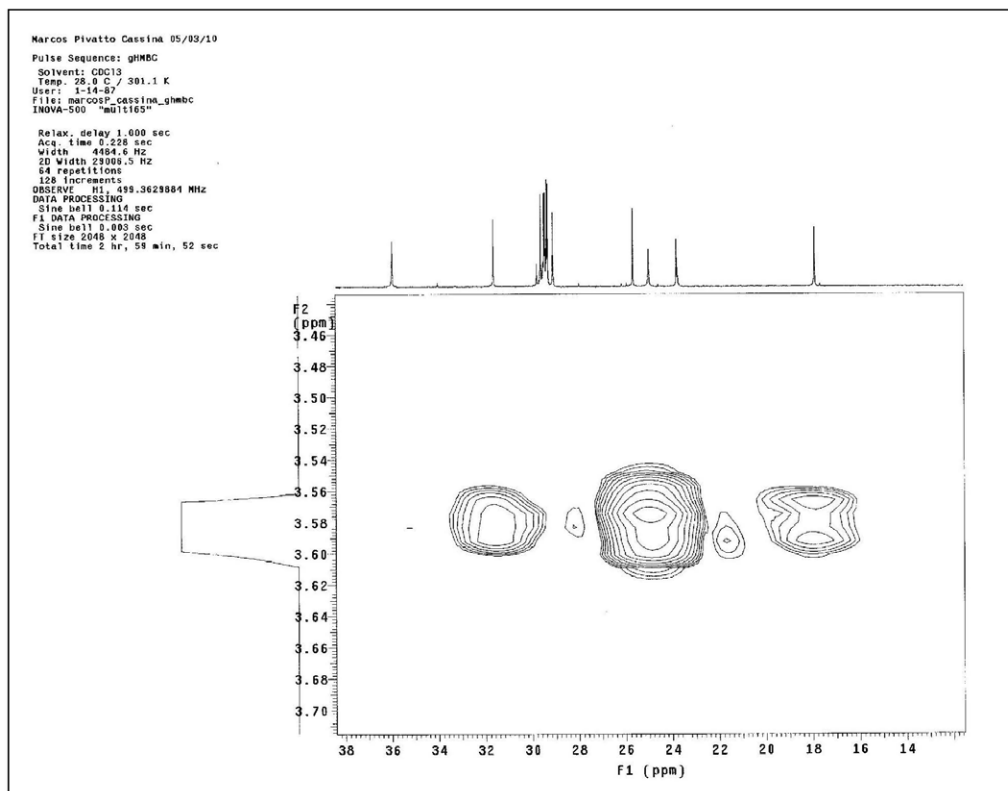
**Figure S26.** HMBC spectrum (expansion δ 14-38) of **1** in chloroform-*d*.
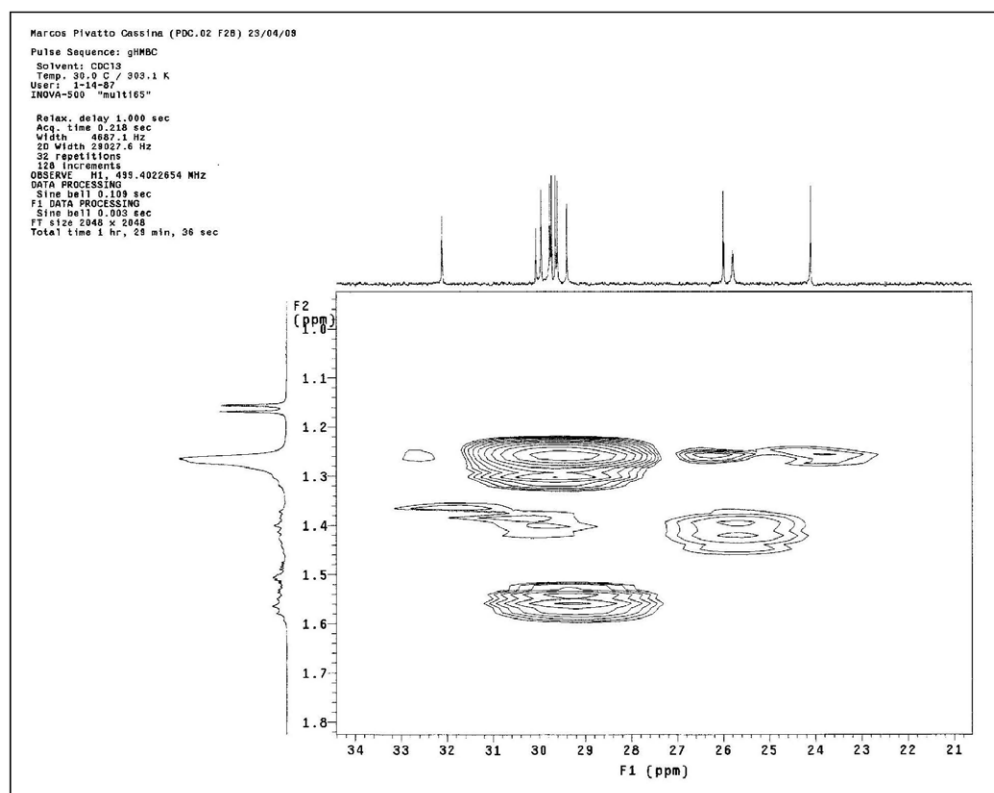
Figure S27. HMBC spectrum (expansion δ 21-34) of **1** in chloroform-*d*.
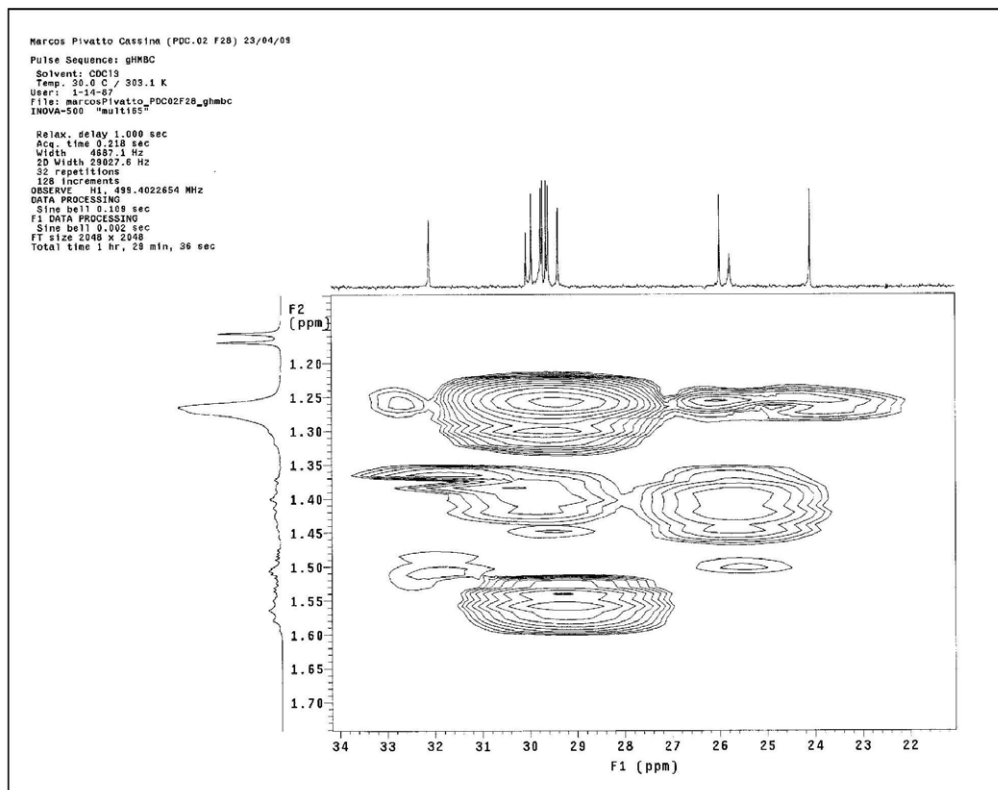
Figure S28. HMBC spectrum (expansion δ 22-34) of **1** in chloroform-*d*.
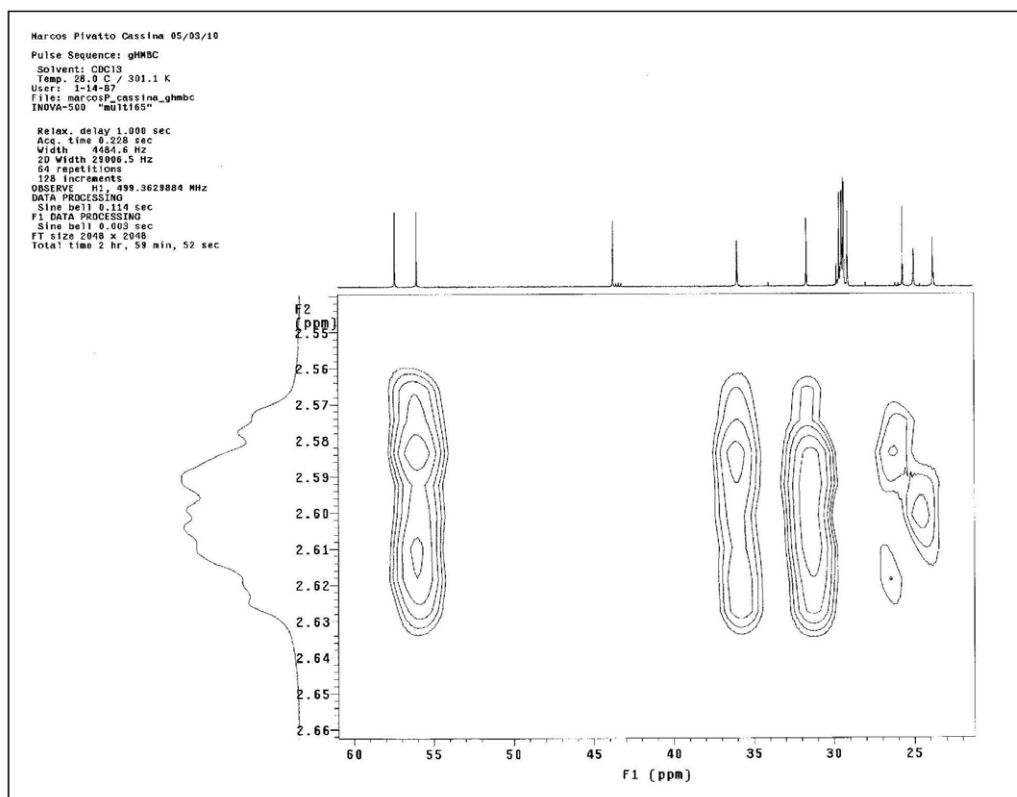
Figure S29. HMBC spectrum (expansion δ 25-60) of **1** in chloroform-*d*.
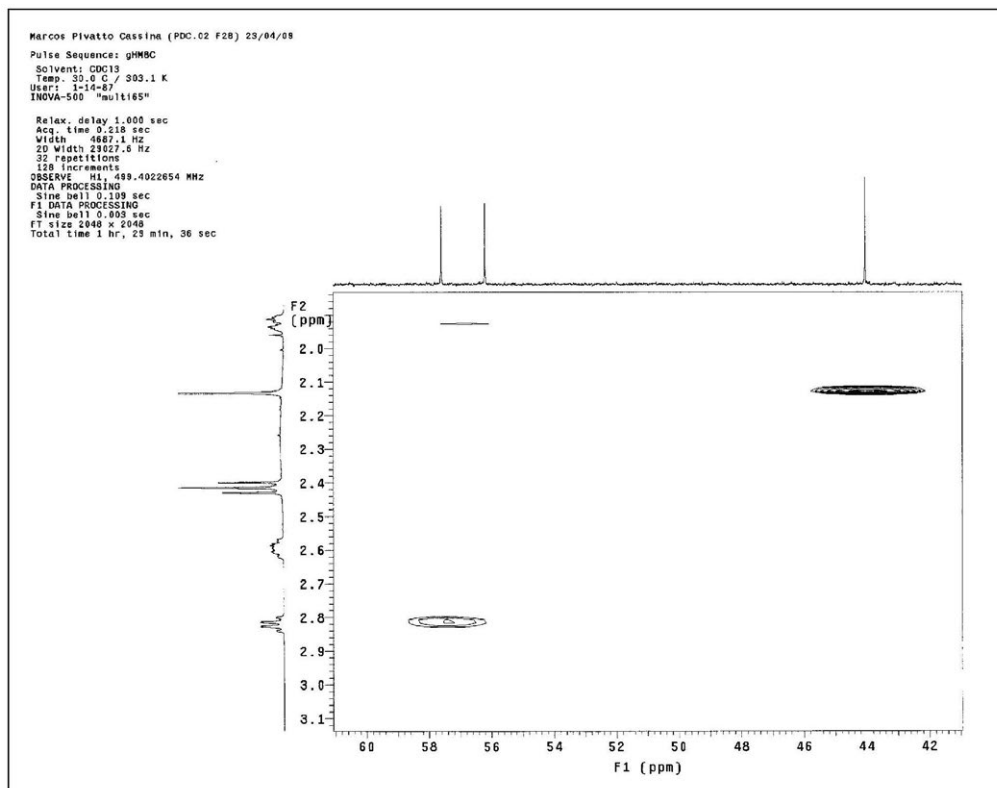
Figure S30. HMBC spectrum (expansion δ 42-60) of **1** in chloroform-*d*.
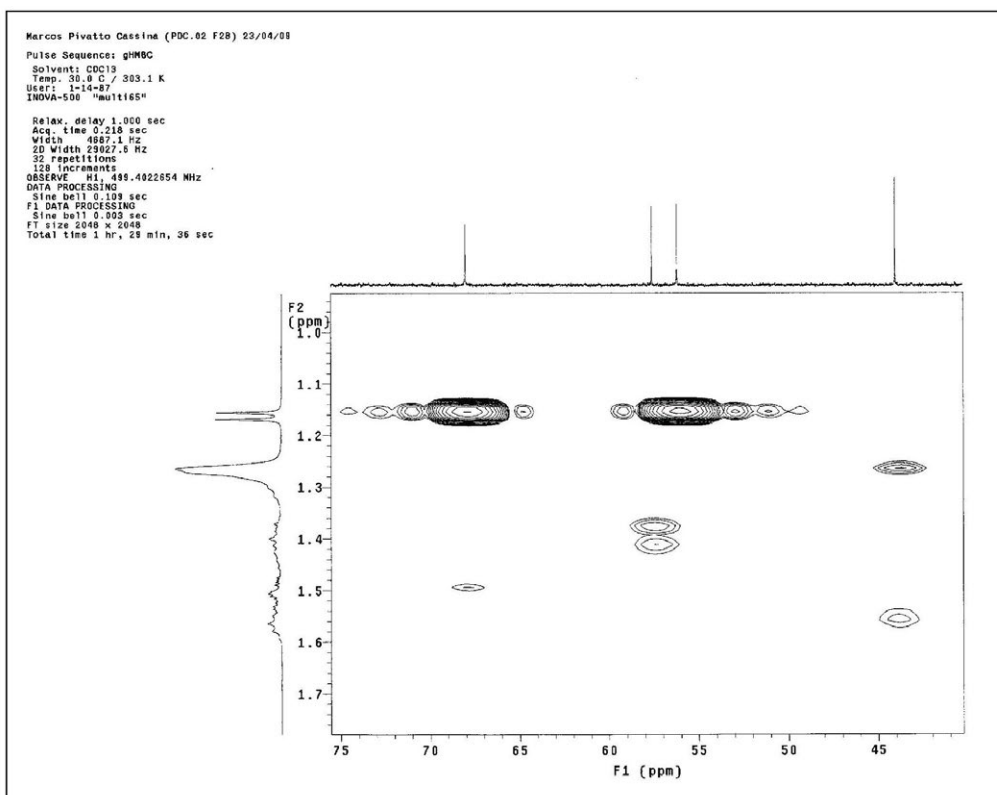
Figure S31. HMBC spectrum (expansion δ 45-75) of **1** in chloroform-*d*.

Figure S32. HMBC spectrum (expansion δ 54-72) of **1** in chloroform-*d*.

Figure S33. HMBC spectrum (expansion δ 198-222) of **1** in chloroform-*d*.
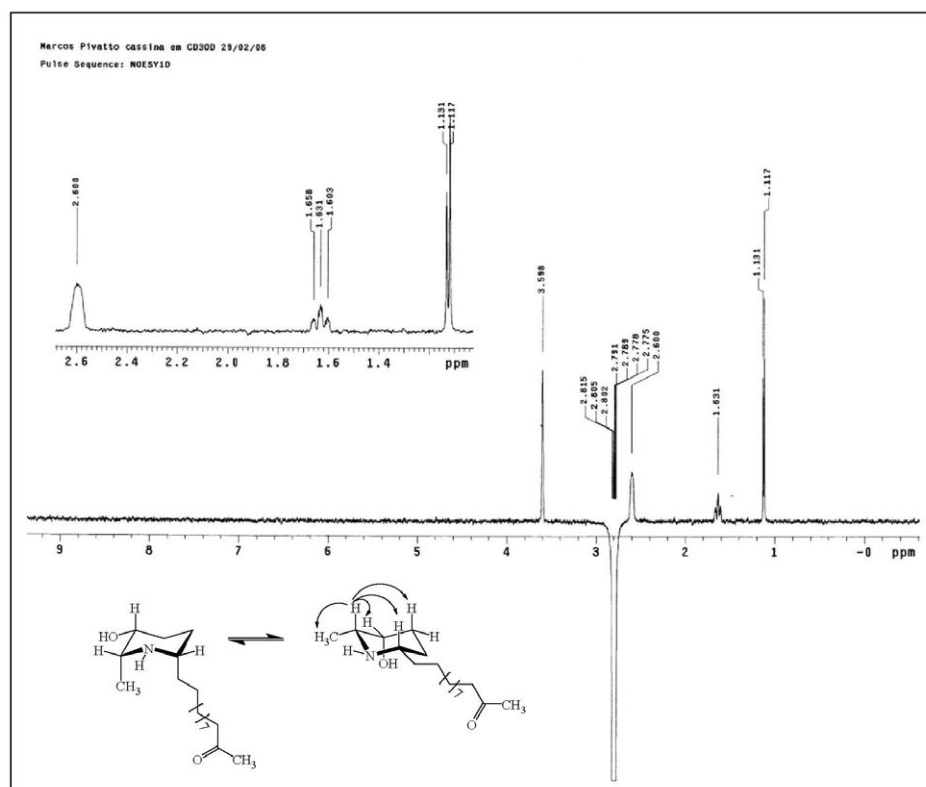
Figure S34. 1D NOESY spectrum of **1** in methanol-*d*$_4$ irradiating δ 2.82.
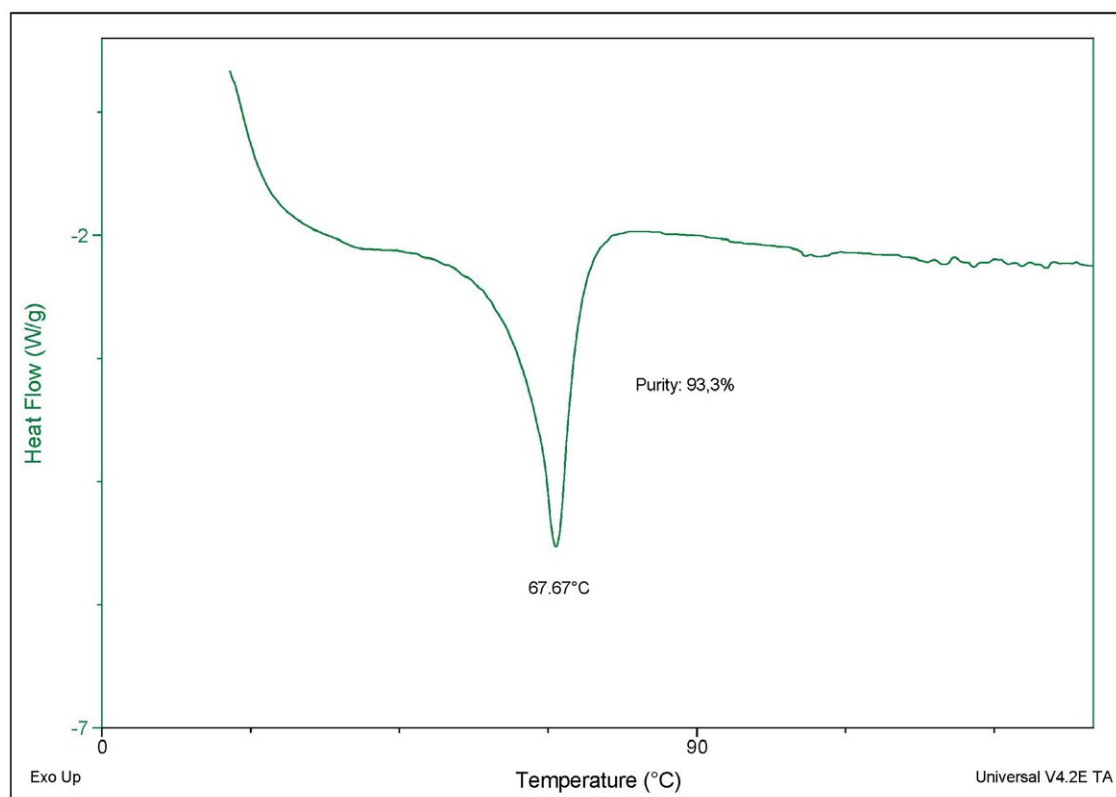
Figure S35. DSC analysis of **2**.
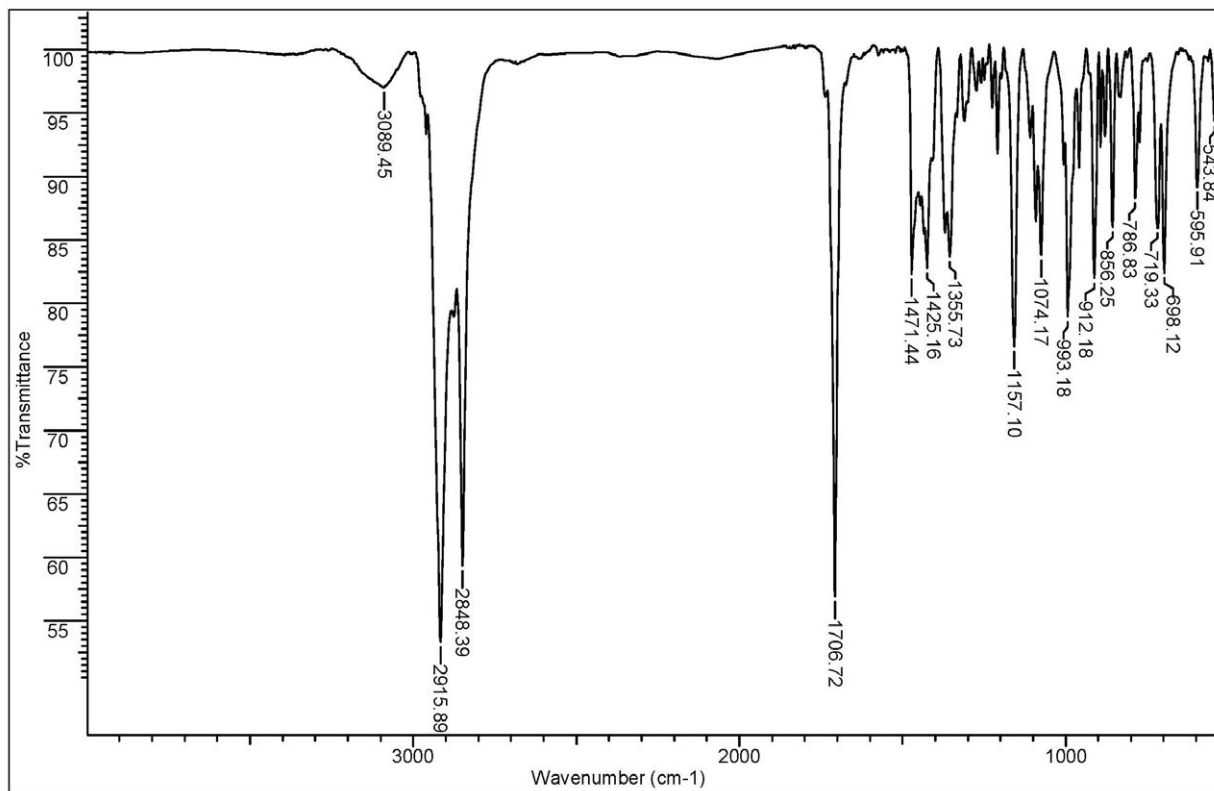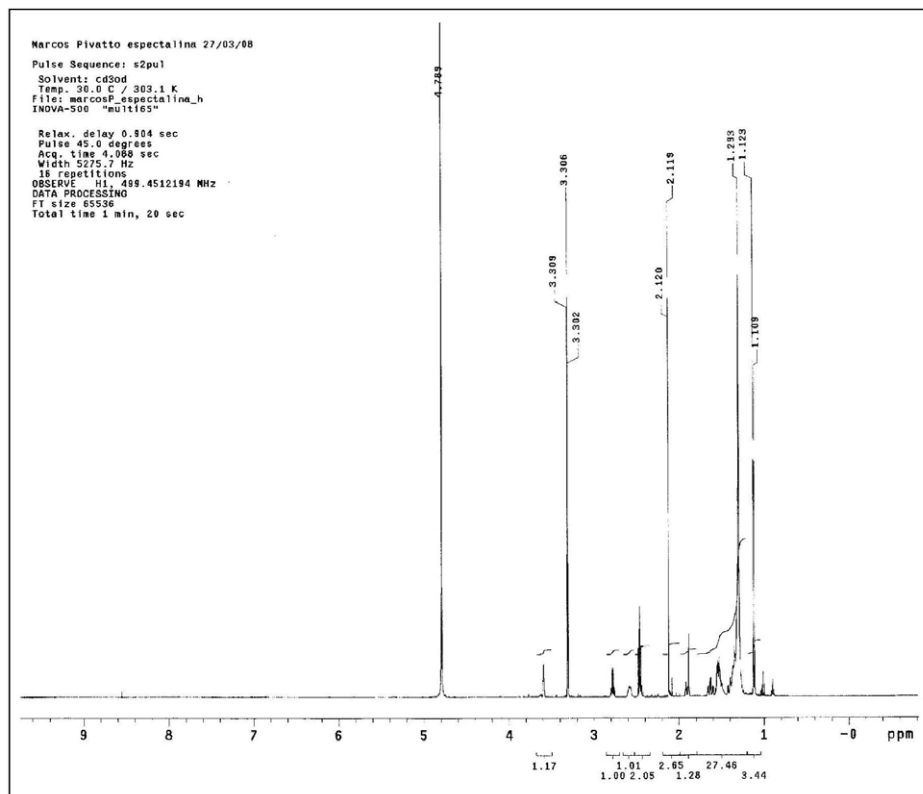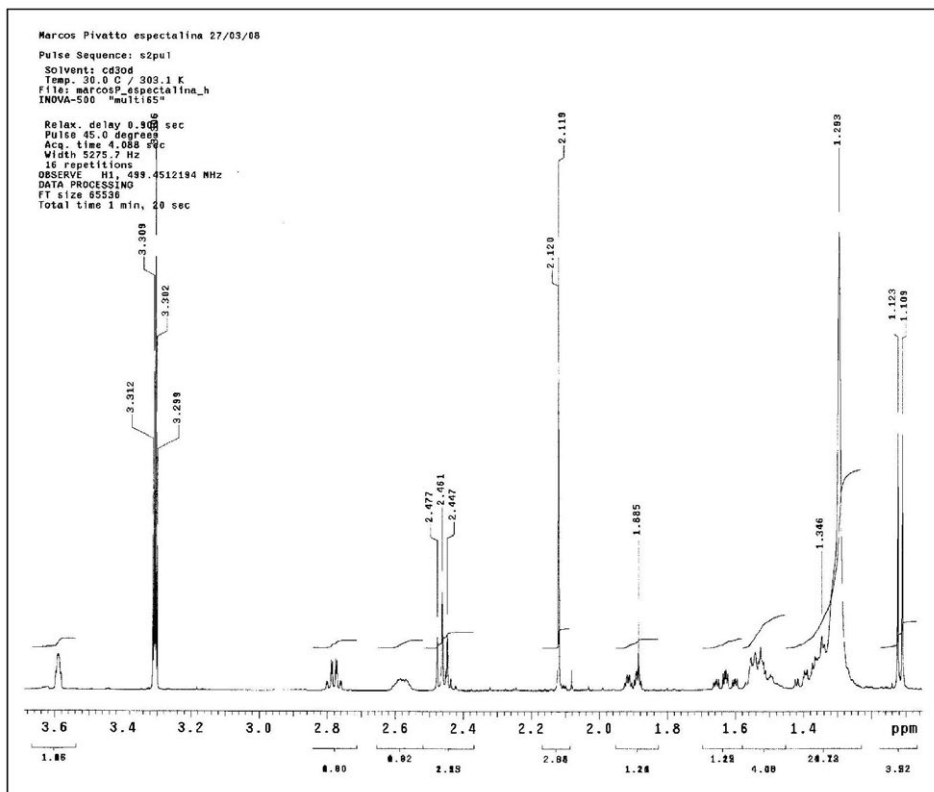
Figure S36. IR spectrum (film) of **2**.
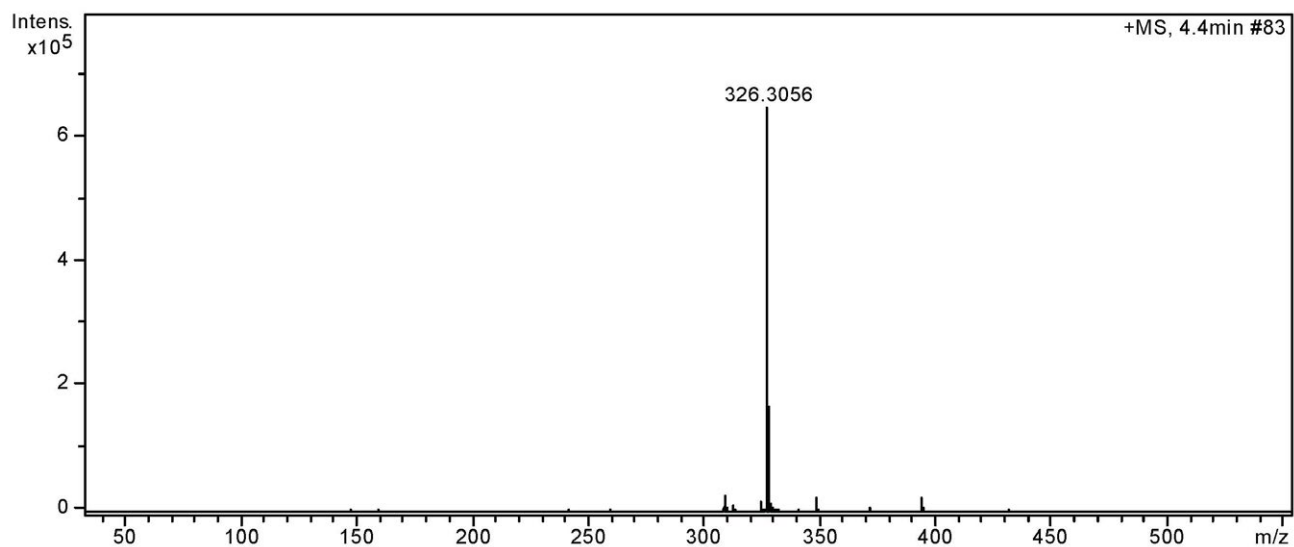
Figure S37. ESI-MS of **2** (HRMS *m/z* 326.3056 [M + H]$^+$ (calcd for $C_{20}H_{40}NO_2$: 326.3054)).

Figure S38. 500 MHz ¹H NMR spectrum of **2** in methanol-d_4.

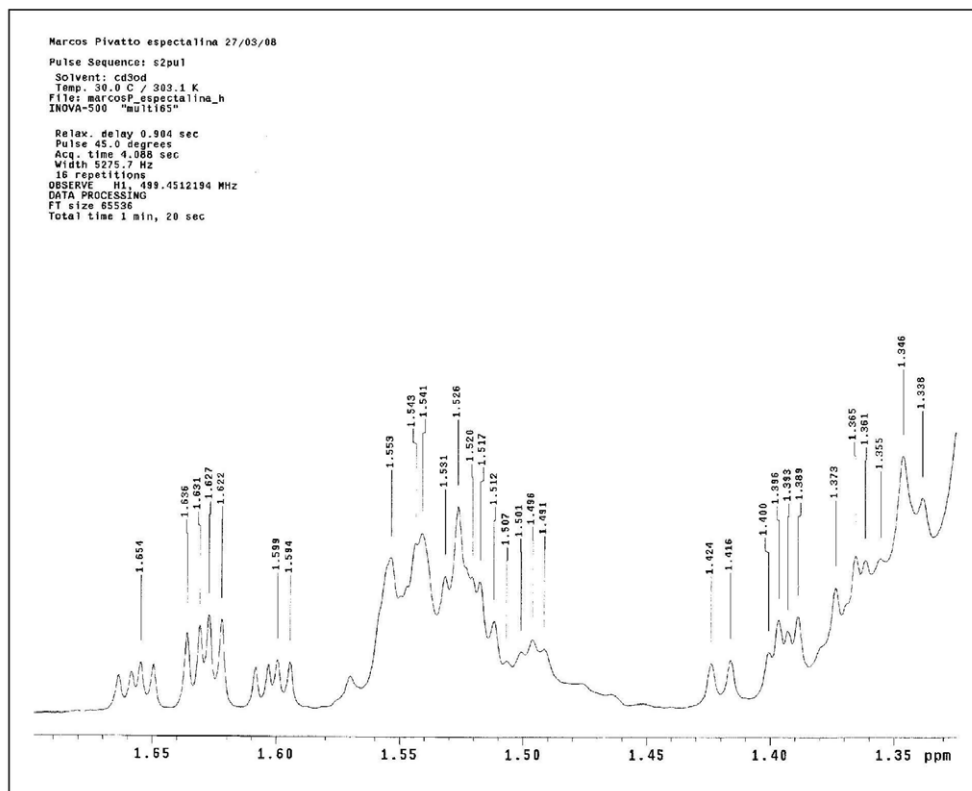**Figure S39.** 500 MHz ¹H NMR spectrum (expansion δ 1.2-3.6) of **2** in methanol-d_4.

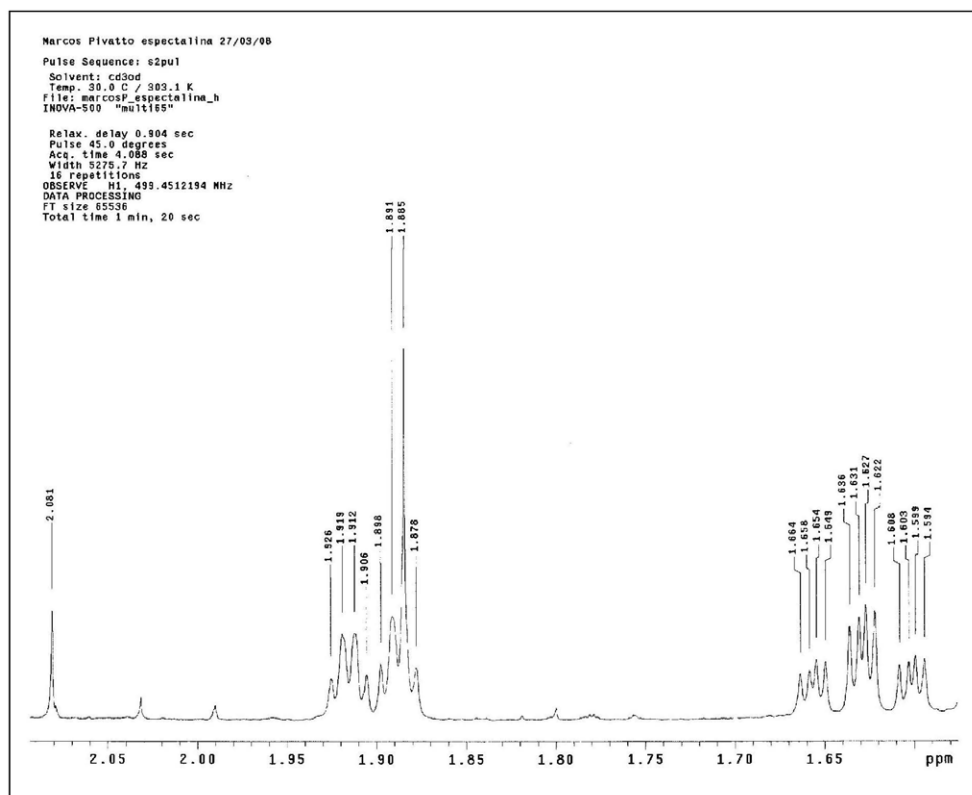**Figure S40.** 500 MHz ^{1}H NMR spectrum (expansion δ 1.35-1.65) of **2** in methanol-d_4.

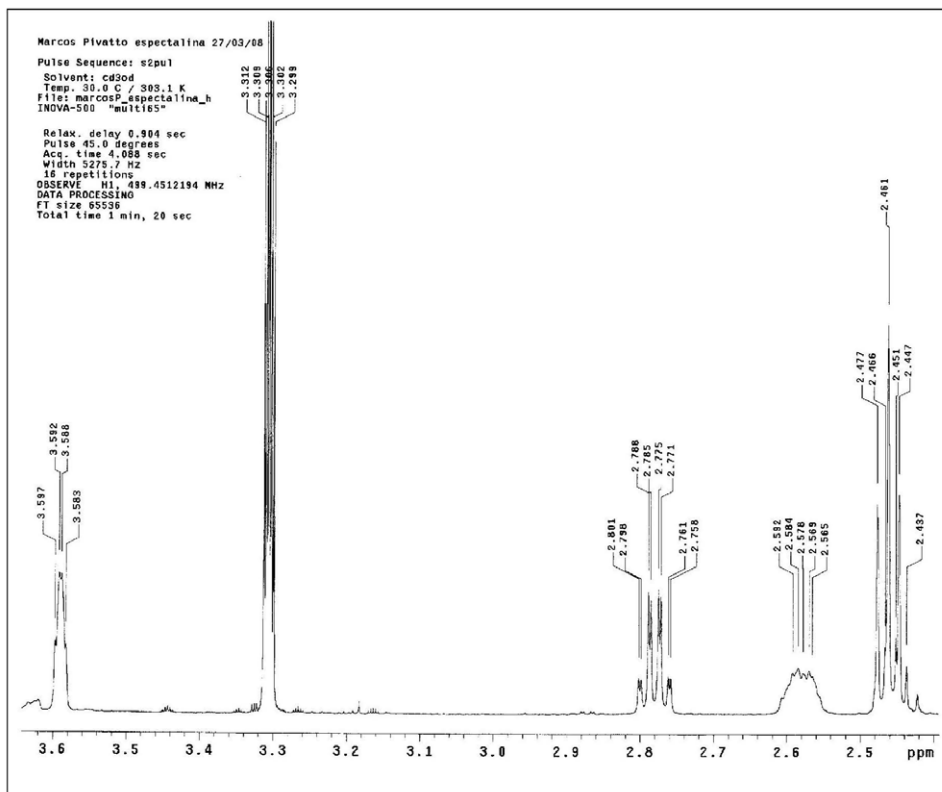**Figure S41.** 500 MHz ^{1}H NMR spectrum (expansion δ 1.60-2.05) of **2** in methanol-d_4.

Figure S42. 500 MHz ^{1}H NMR spectrum (expansion δ 2.4-3.6) of **2** in methanol-d_4.
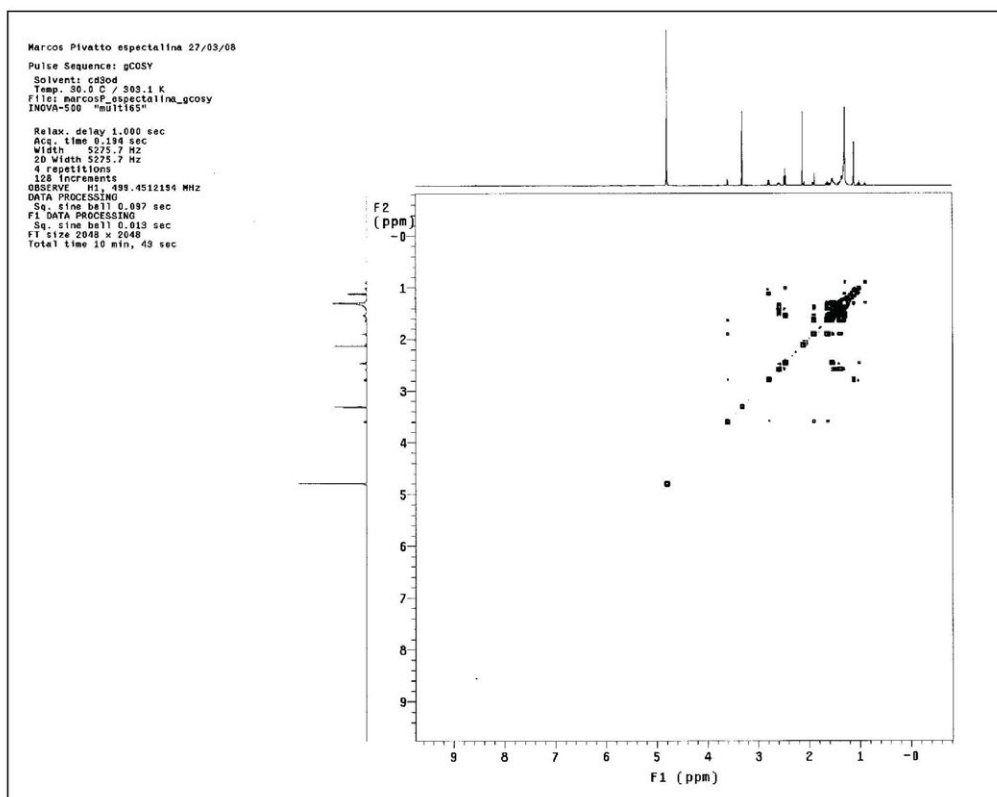

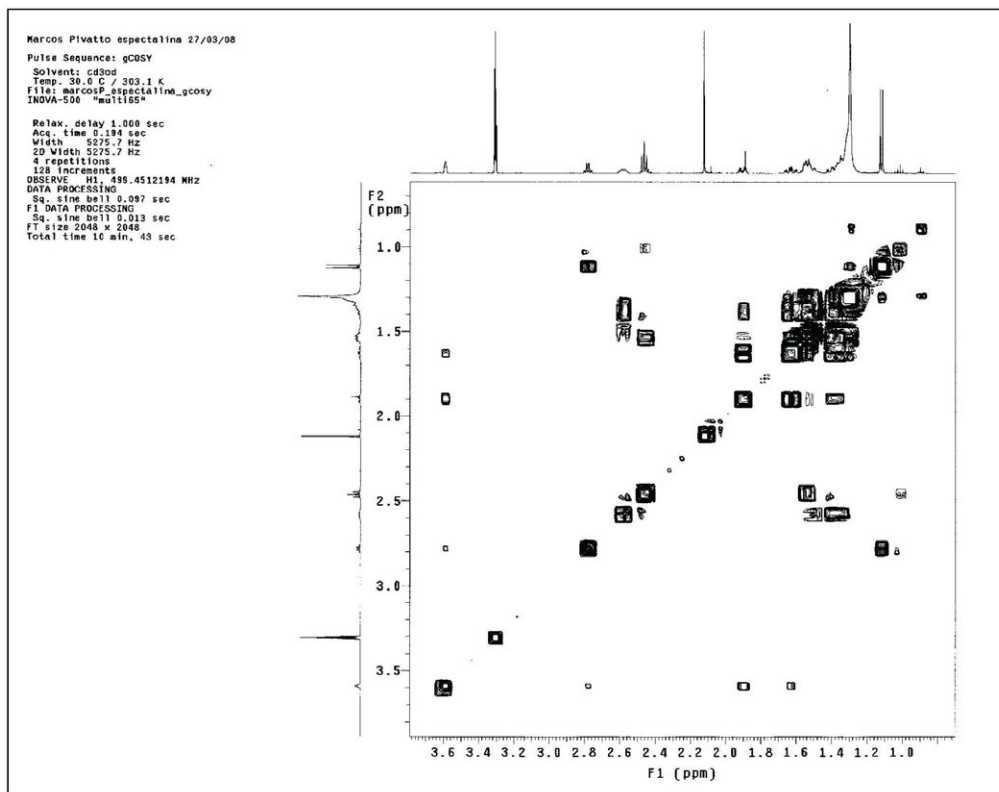**Figure S43.** COSY spectrum of **2** in methanol-d_4.

Figure S44. COSY spectrum (expansion δ 0.0-3.6) of **2** in methanol-d_4.
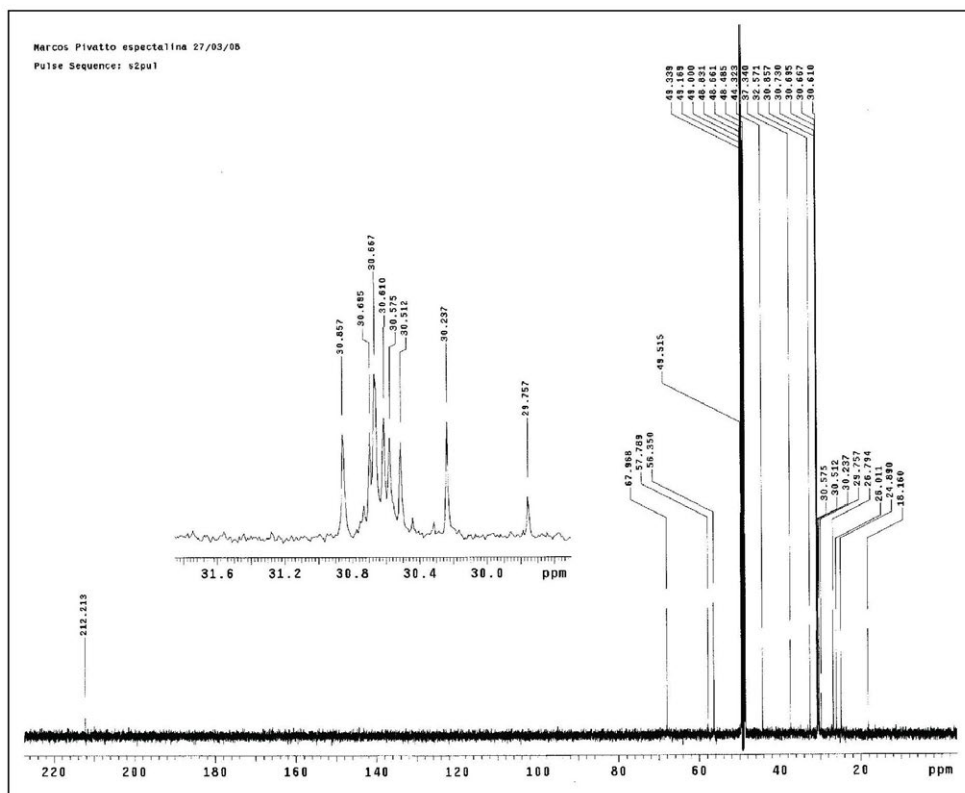

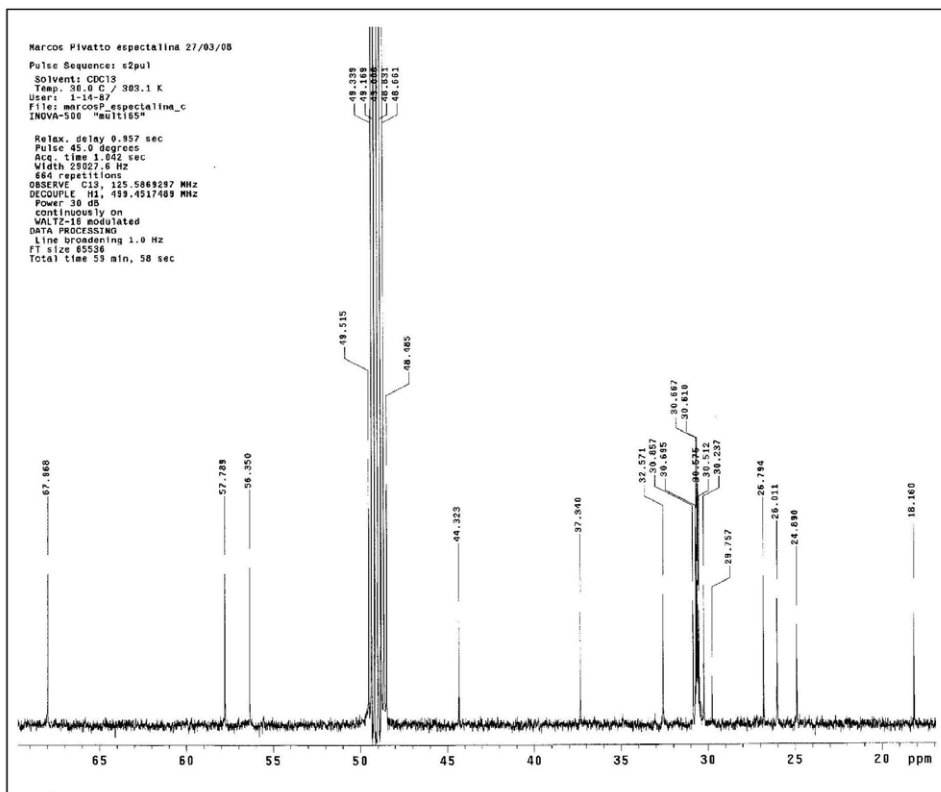**Figure S45.** 125 MHz ^{13}C NMR spectrum of **2** in methanol-d_4.

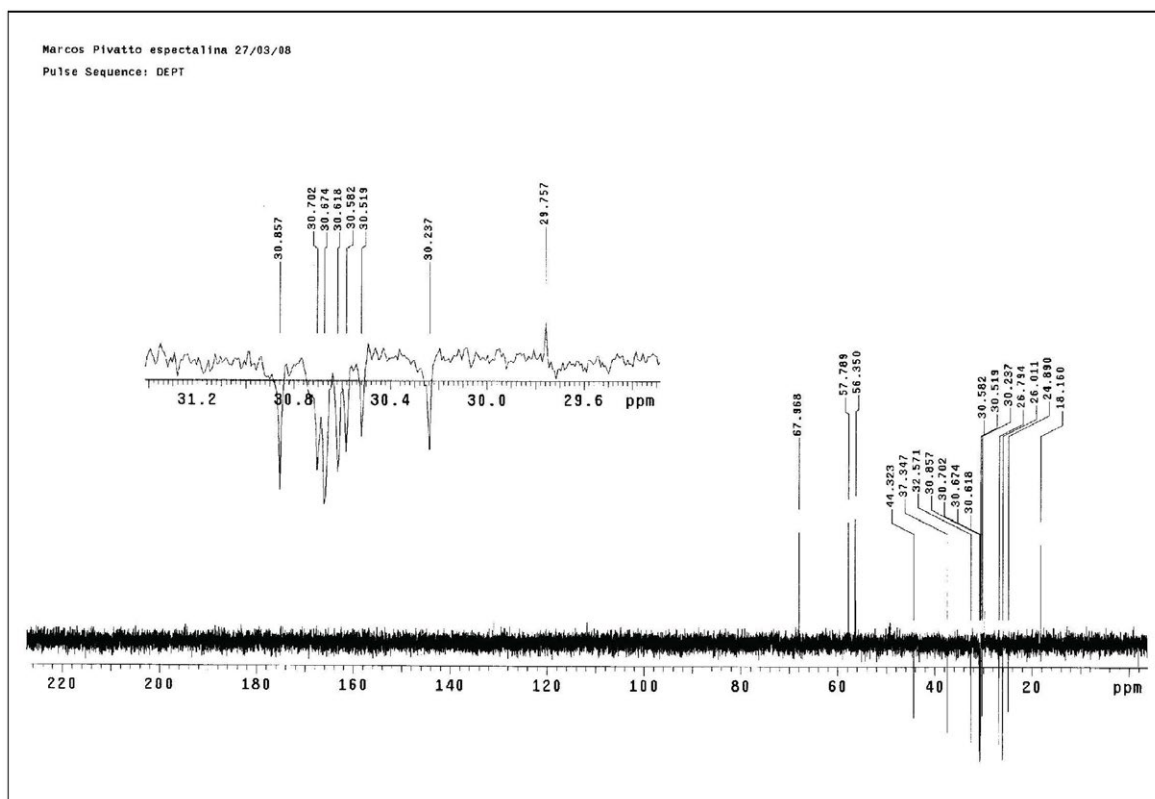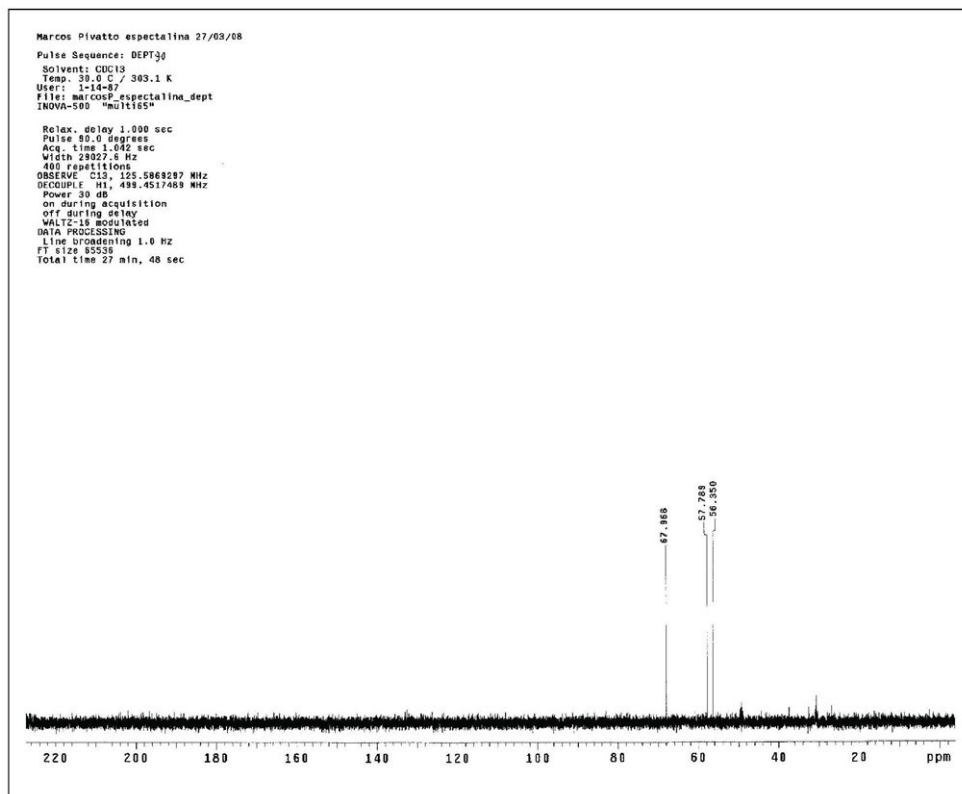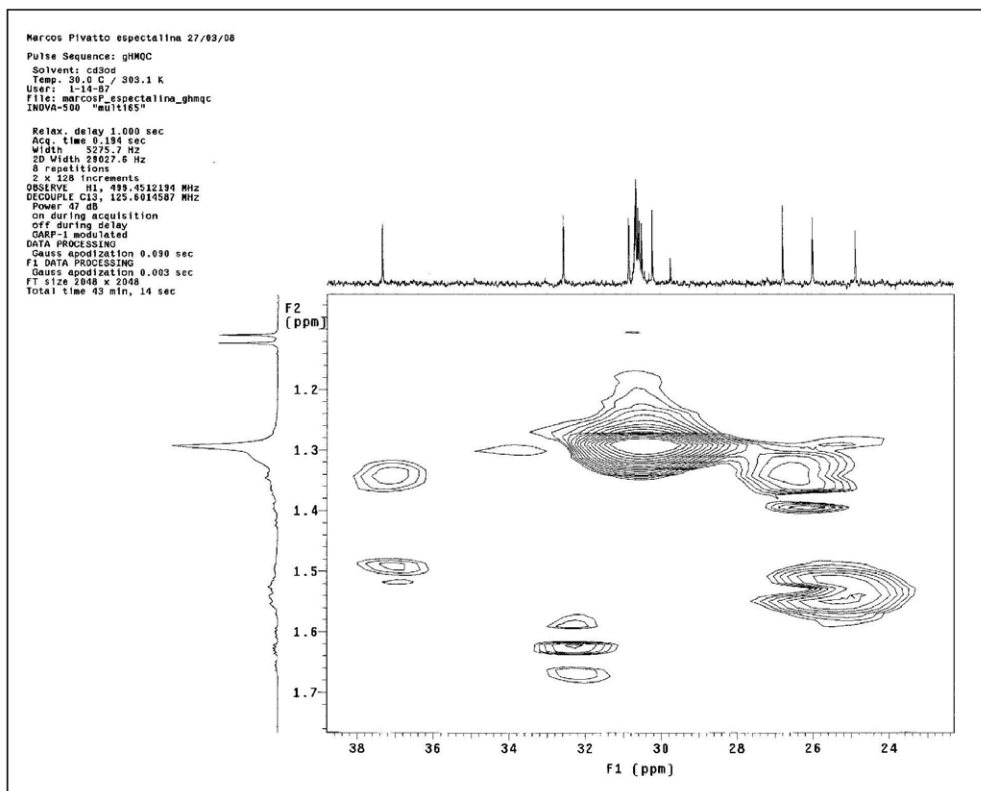**Figure S46.** 125 MHz ¹³C NMR spectrum (expansion δ 20-65) of **2** in methanol-d_4.

Figure S47. 125 MHz DEPT 135 NMR spectrum of **2** in methanol-d_4.

Marcos Pivatto espectalina 27/03/08

Pulse Sequence: DEPT 90

Solvent: CDCl3
Temp. 30.0 C / 303.1 K
User: 1-14-87
File: marcosP_espectalina_dept
INOVA-500 "multi65"

Relax. delay 1.000 sec
Pulse 90.0 degrees
Acq. time 1.042 sec
Width 29027.6 Hz
400 repetitions
OBSERVE C13, 125.5869287 MHz
DECOUPLE H1, 499.4517469 MHz
Power 30 dB
on during acquisition
off during delay
WALTZ-16 modulated
DATA PROCESSING
Line broadening 1.0 Hz
FT size 65536
Total time 27 min, 48 sec

Figure S48. 125 MHz DEPT 90 NMR spectrum of **2** in methanol-d_4.

Marcos Pivatto espectalina 27/03/08

Pulse Sequence: gHMQC

Solvent: cd3od
Temp. 30.0 C / 303.1 K
User: 1-14-87
File: marcosP_espectalina_ghmqc
INOVA-500 "multi65"

Relax. delay 1.000 sec
Acq. time 0.194 sec
Width 5275.7 Hz
2D Width 29027.6 Hz
8 repetitions
2 x 128 increments
OBSERVE H1, 499.4512194 MHz
DECOUPLE C13, 125.6014587 MHz
Power 47 dB
on during acquisition
off during delay
GARP-1 modulated
DATA PROCESSING
Gauss apodization 0.090 sec
F1 DATA PROCESSING
Gauss apodization 0.003 sec
FT size 2048 x 2048
Total time 43 min, 14 sec

Figure S49. HMQC spectrum of **2** in methanol-d_4.

Figure S50. HMQC spectrum (expansion δ 24-38) of **2** in methanol-d_4.
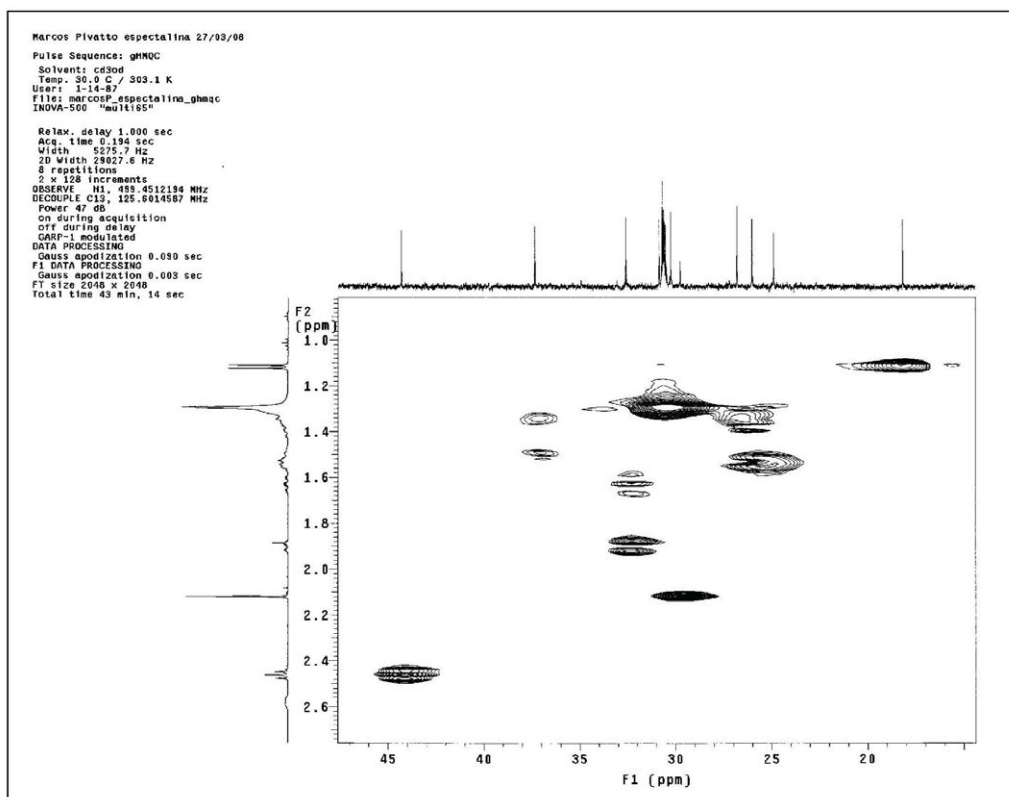
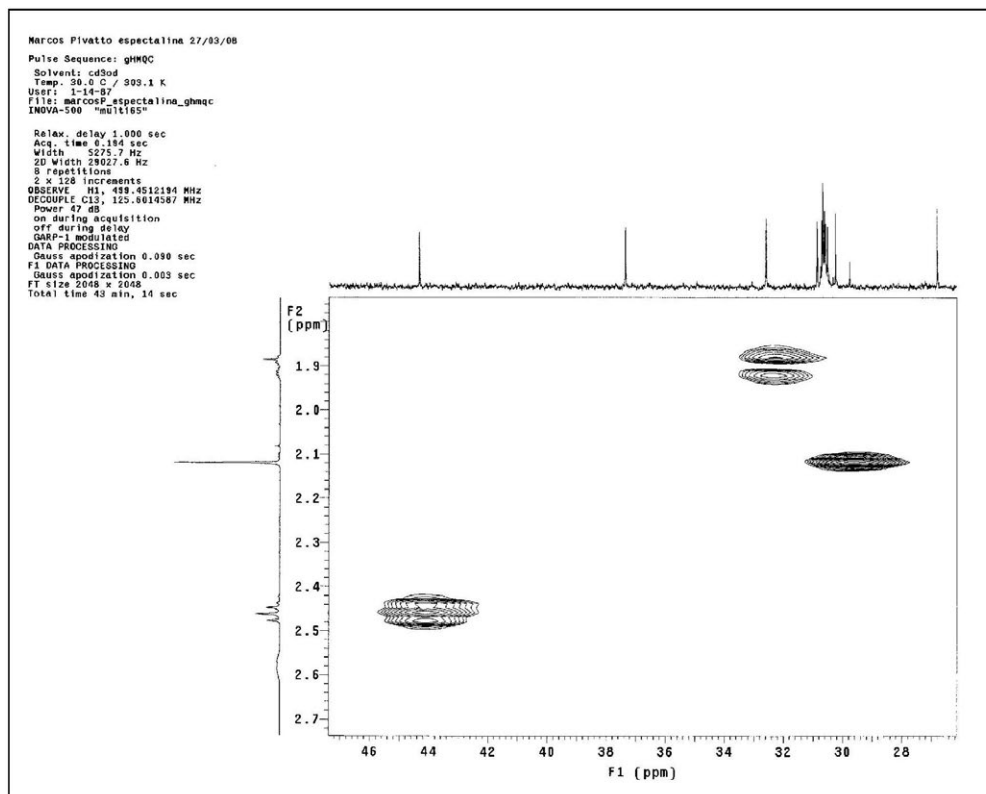**Figure S51.** HMQC spectrum (expansion δ 20-45) of **2** in methanol-d_4.

Figure S52. HMQC spectrum (expansion δ 28-46) of **2** in methanol-d_4.
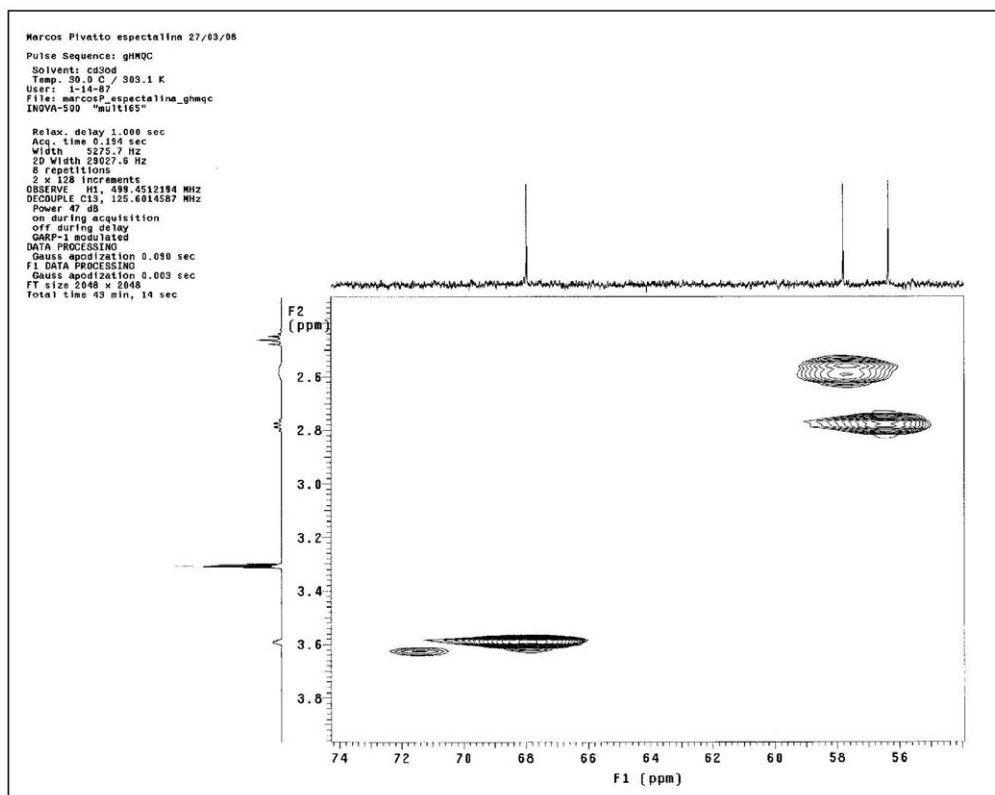

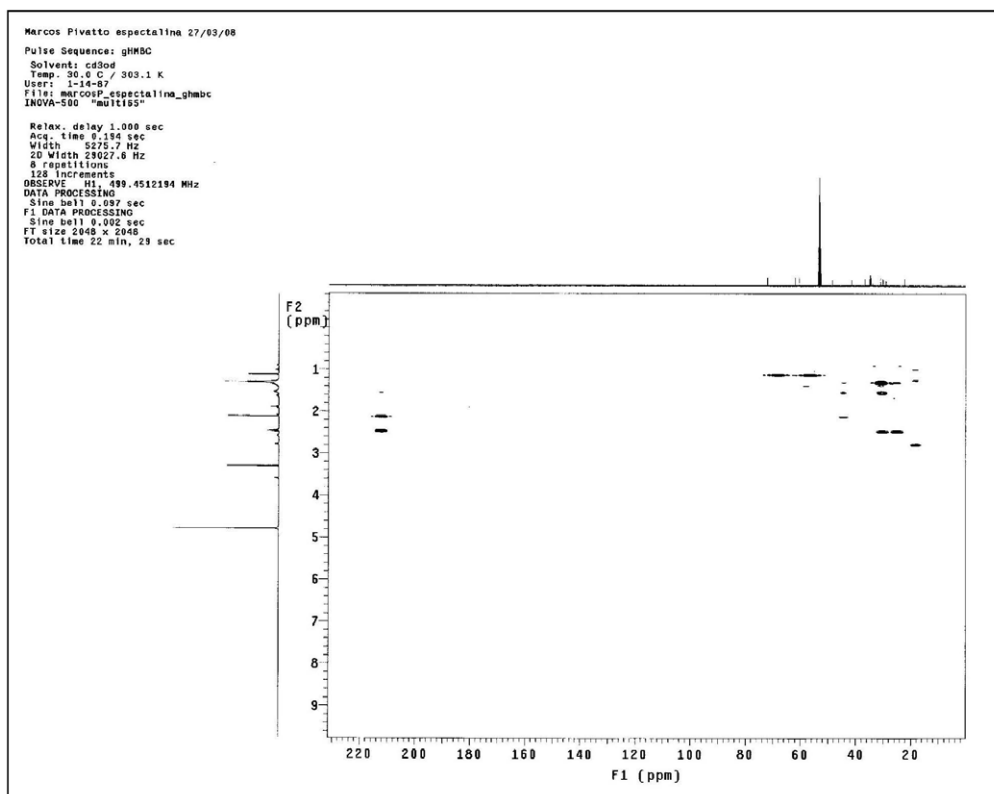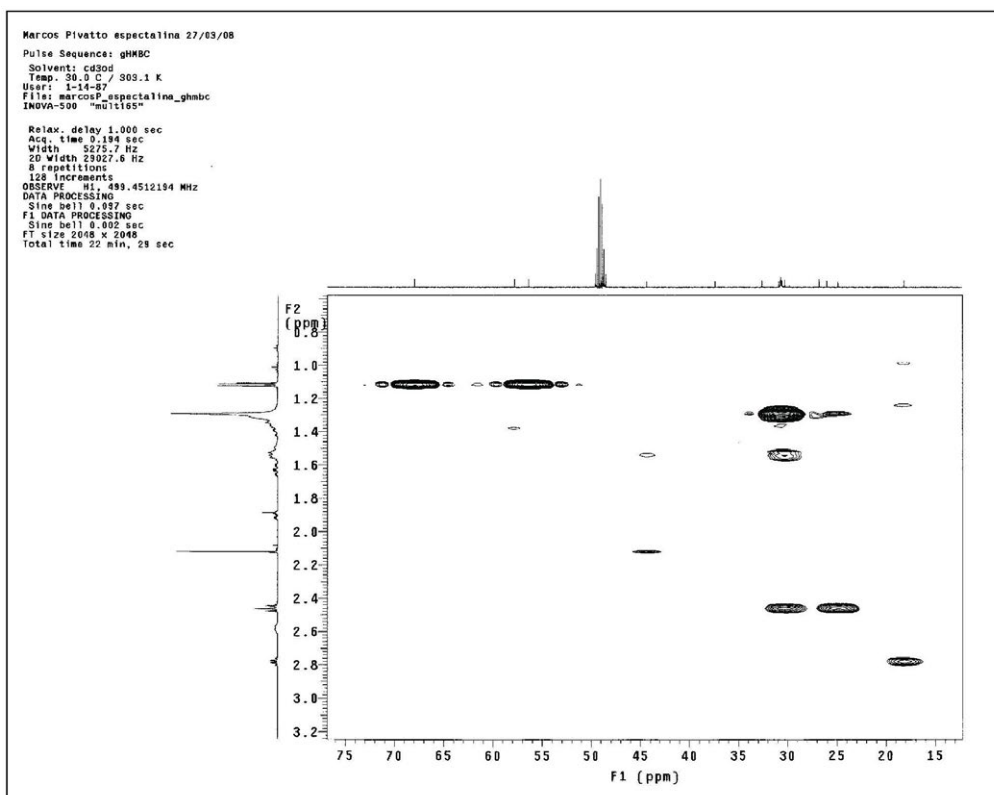**Figure S53.** HMQC spectrum (expansion δ 54-74) of **2** in methanol-d_4.

Figure S54. HMBC spectrum of **2** in methanol-d_4.

Figure S55. HMBC spectrum (expansion δ 15-75) of **2** in methanol-d_4.
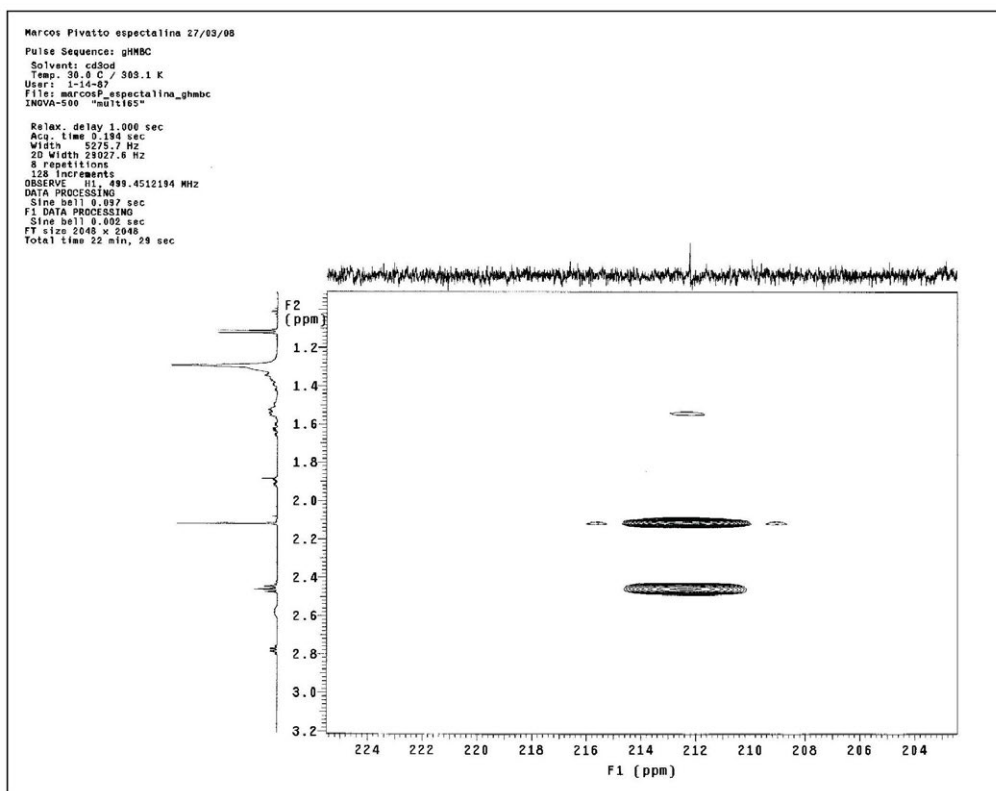
Figure S56. HMBC spectrum (expansion δ 204-224) of **2** in methanol-d_4.
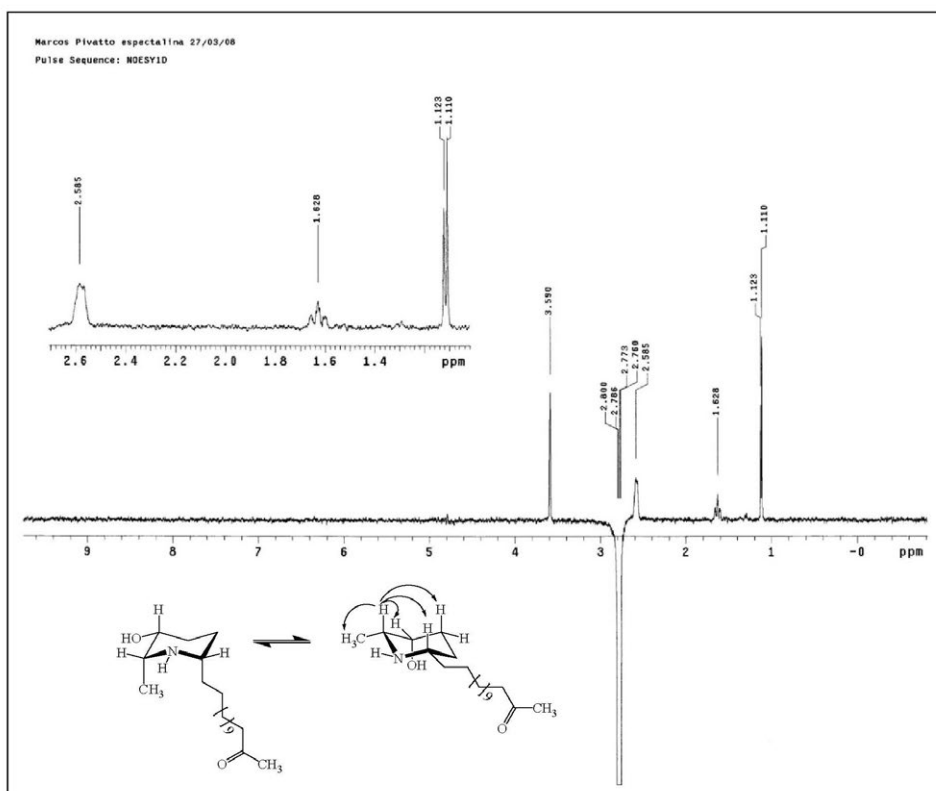
Figure S57. 1D NOESY spectrum of **2** in methanol-d_4 irradiating δ 2.78.

Figure S58. TLC (SiO$_2$) of **3** (A: free base, B: hydrochloride) and **4** (C: free base, D: hydrochloride) developed with CHCl$_3$-MeOH-NH$_4$OH (9:1:0.25) and revealed with iodochloroplatinate reagent.
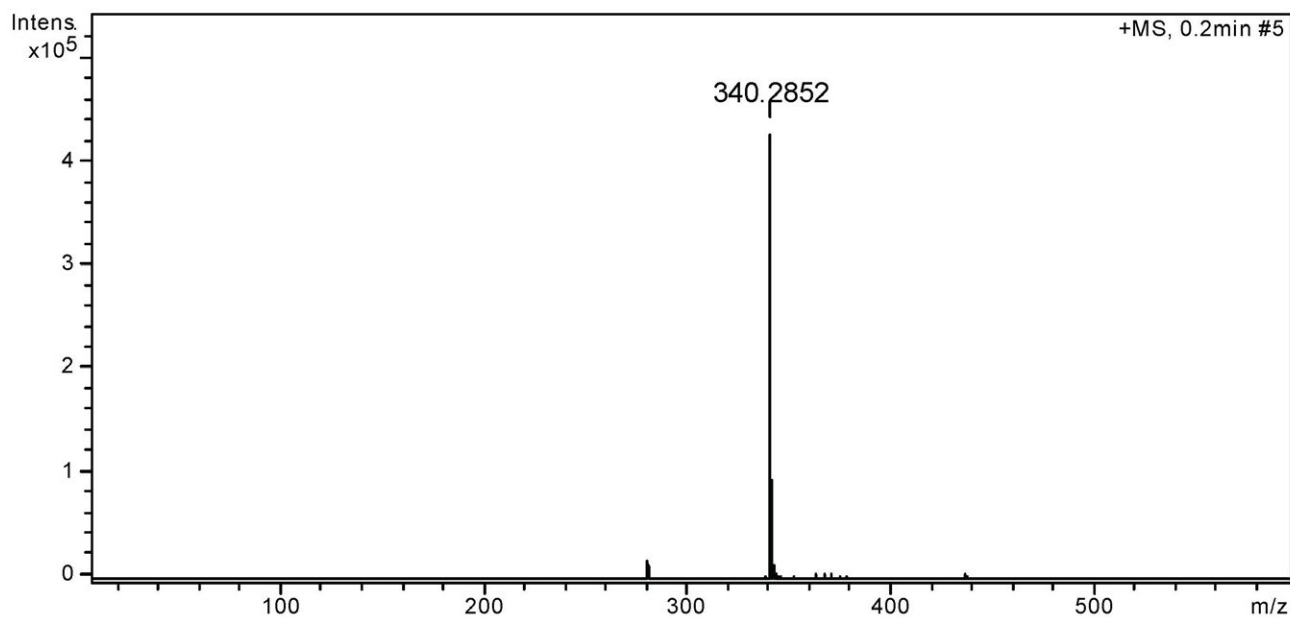
Figure S59. ESI-MS of **2** (HRMS *m/z* 340.2852 [M + H]$^+$ (calcd for C$_{20}$H$_{40}$NO$_2$: 340.2852)).
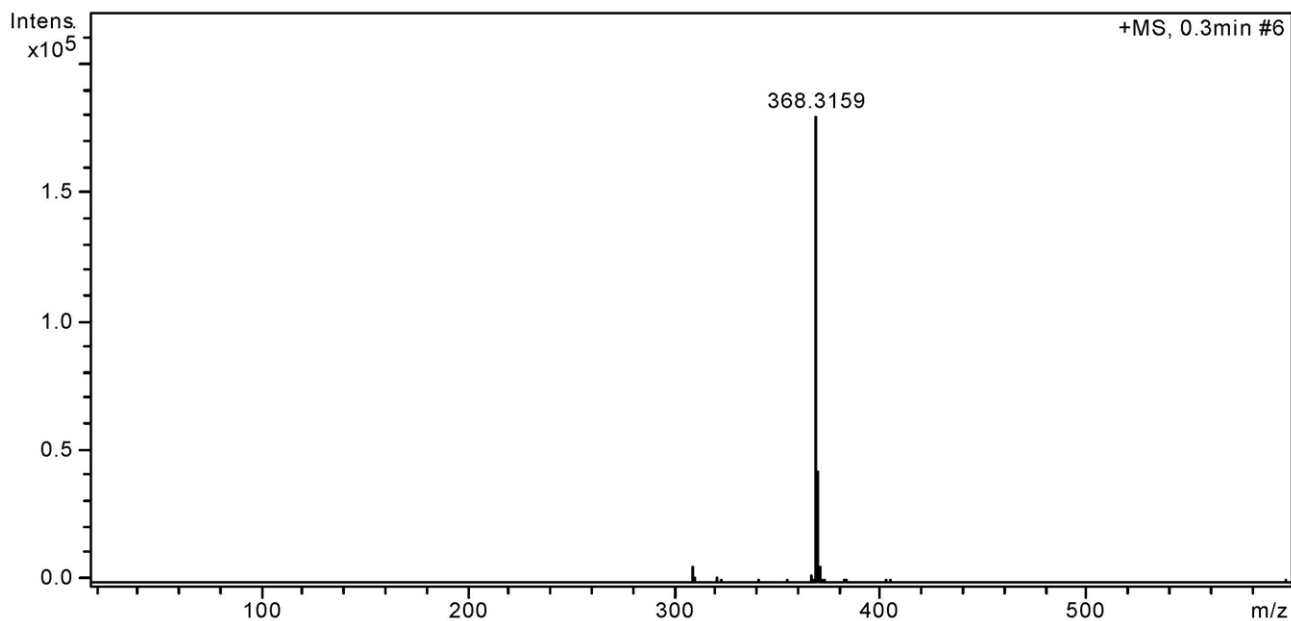
Figure S60. ESI-MS of **2** (HRMS *m/z* 368.3159 [M + H]$^+$ (calcd for $C_{20}H_{40}NO_2$: 368.3165)).

Figure S61. Modified Kipp's apparatus.

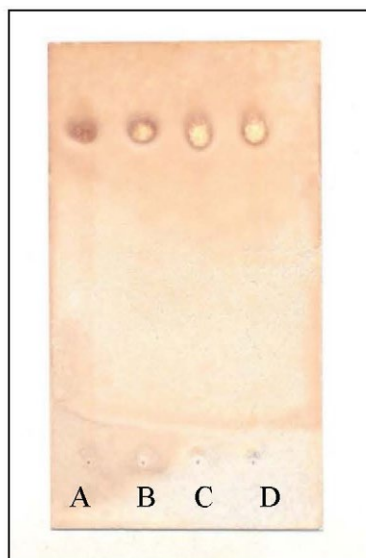**Table S1.** Data to plot graph of the antimalarial activity of (−)-cassine (**1**) (IC$_{50}$ 1.82 μM)

Concentration / M	Mean survival / %			Standard deviation
	Experiment 1	Experiment 2	Experiment 3	
0.000000001	107.2505	100.8985	105.1969	3.241435369
0.00000001	104.8964	98.56245	104.252	3.485808208
0.0000001	100.9416	94.51932	100.0787	3.485612878
0.000001	84.27496	78.34681	84.80315	3.584835498
0.00001	39.17138	39.1734	48.97638	5.660336356
0.0001	28.15442	39.3531	54.48819	13.21582905

Table S2. Data to plot graph of the antimalarial activity of (–)-spectaline (**2**) (IC_{50} 2.76 μM)

Concentration / M	Mean survival / %			Standard deviation
	Experiment 1	Experiment 2	Experiment 3	
0.000000001	99.81413	107.9892	95.7431	6.236613
0.00000001	102.881	97.12747	99.25317	2.909263
0.0000001	114.4052	95.51167	111.6505	10.20634
0.000001	89.68401	90.0359	86.78118	1.786218
0.00001	44.42379	43.62657	47.94623	2.298645
0.0001	40.61338	32.58528	48.17028	7.793687

Table S3. Data to plot graph of the antimalarial activity of (–)-3-*O*-acetylcassine (**3**) (IC_{50} 24.47 μM)

Concentration / M	Mean survival / %			Standard deviation
	Experiment 1	Experiment 2	Experiment 3	
1.28×10^{-09}	90.54	85.65	73.32	8.873832
6.40×10^{-09}	92.63	87.76	69.74	12.05812
3.20×10^{-08}	80.18	79.23	67.709	6.942163
1.60×10^{-07}	84	78.43	68.72	7.73291
0.0000008	84.81	78.43	66.92	9.066758
0.000004	82.63	72.11	57.623	12.55583
0.00002	73.54	58.17	38.85	17.38244
0.0001	45.818	38.31	21.18	12.62826

Table S4. Data to plot graph of the antimalarial activity of (–)-3-*O*-acetylspectaline (**4**) (IC_{50} 25.14 μM)

Concentration / M	Mean survival / %			Standard deviation
	Experiment 1	Experiment 2	Experiment 3	
1.28×10^{-09}	89.09	88.86	73.96	8.669677
6.40×10^{-09}	91.63	88.46	68.96	12.27618
3.20×10^{-08}	90.63	92.27	68.1	13.50604
1.60×10^{-07}	85.9	90.07	67.005	12.29095
0.0000008	80.18	81.54	62.392	10.68417
0.000004	88.36	74.52	58.092	15.15243
0.00002	69.45	54.56	38.15	15.65615
0.0001	40.27	38.61	12.9	15.34534

Table S5. Data to plot graph of the antimalarial activity of chloroquine (IC_{50} 0.30 μM)

Concentration / M	Mean survival / %			Standard deviation
	Experiment 1	Experiment 2	Experiment 3	
1.28×10^{-09}	94	84.18	95.75	6.23644931
6.40×10^{-09}	84.22274	84.27	94.96	6.1855623
3.20×10^{-08}	84.57076	80.45	88.67	4.110004695
1.60×10^{-07}	71.34571	67.63	87.88	10.78001041
0.0000008	48.14385	36.9	45.08	5.81268354
0.000004	46.98376	41.9	44.21	2.545403055
0.00002	29.00232	32.81	43.27	7.387790824
0.0001	17.74942	38.36	40.51	12.56624122